



# Urban Air Mobility Longitudinal Flight Transition Control for VTOL Aircraft

Versão final após defesa

Ana Isabel Chitas Pires Belas

Dissertação para obtenção do Grau de Mestre em **Engenharia  
Aeronáutica**  
(Ciclo de estudos integrado)

Orientador:  
Prof. Doutor Kouamana Bousson

Covilhã, Abril de 2024



# Declaração de Integridade

Eu, Ana Belas, que abaixo assino, estudante com o número de inscrição 41421 de Engenharia Aeronáutica da Faculdade de Engenharia, declaro ter desenvolvido o presente trabalho e elaborado o presente texto em total consonância com o **Código de Integridades da Universidade da Beira Interior**.

Mais concretamente afirmo não ter incorrido em qualquer das variedades de Fraude Académica, e que aqui declaro conhecer, que em particular atendi à exigida referenciação de frases, extratos, imagens e outras formas de trabalho intelectual, e assumindo assim na íntegra as responsabilidades da autoria.

*Ana Belas*

Universidade da Beira Interior, Covilhã 15/4/2024



# Acknowledgments

This dissertation encapsulates a profound sense of achievement, and it has been a distinct honor to navigate the intellectual corridors of this esteemed university. I extend sincere gratitude to UBI, not only for the wealth of academic knowledge bestowed upon me but also for the invaluable life lessons that will resonate throughout my journey.

A special acknowledgment is reserved for Professor Dr. Kouamana Bousson, a beacon of inspiration for many students. His constant availability, guidance, and impactful contributions have been pivotal in shaping the trajectory of this work.

My heartfelt appreciation extends to my entire family, with special mention to my parents, Mariete and José, whose unwavering support, sacrifices, and encouragement have been my steadfast companions on this journey. They are my unyielding pillar of strength. To my friends, I express deep thanks for their unwavering support, serving as a wellspring of motivation during critical junctures.

I am also grateful to my colleagues at Honeywell, Czech Republic, for their patience and flexibility, facilitating a harmonious balance between work commitments and the successful completion of this thesis.



# Acronyms

**EASA** European Union Aviation Safety Agency

**FAA** Federal Aviation Administration

**LQR** Linear Quadratic Regulator

**UAM** Urban Air Mobility

**UAV** Unmanned Aerial Vehicle

**UBI** Universidade da Beira Interior (Beira Interior University)

**VTOL** Vertical Take-off and Landing



# Symbols

|                    |  |
|--------------------|--|
| $\infty$           | Infinite   |
| $a$                | acceleration   |
| $\alpha$           | Angle of attack  |
| $C_D$              | Coefficient of Drag  |
| $C_{D_0}$          | Derivative of the Drag coefficient for a null angle of attack            |
| $C_{D_\alpha}$     | Derivative of the Drag coefficient with the angle of attack              |
| $C_{D_{\delta_e}}$ | Derivative of the Drag coefficient with the elevator rate                |
| $C_L$              | Coefficient of Lift  |
| $C_{L_0}$          | Derivative of the Lift coefficient for a null angle of attack            |
| $C_{L_\alpha}$     | Derivative of the Lift coefficient with the angle of attack              |
| $C_{L_{\delta_e}}$ | Derivative of the Lift coefficient with the elevator rate                |
| $C_m$              | Pitching Moment Coefficient  |
| $C_{m_0}$          | Derivative of the Pitching Moment coefficient for a null angle of attack |
| $C_{m_q}$          | Derivative of the Pitching Moment coefficient with the pitch rate        |
| $C_{m_\alpha}$     | Derivative of the Pitching Moment coefficient with the angle of attack   |
| $C_{m_{\delta_e}}$ | Derivative of the Pitching Moment coefficient with the elevator rate     |
| $C_n$              | Coefficient of Yaw Moment  |
| $C_y$              | Coefficient of Sideslip  |
| $\delta_e$         | Elevator rate  |
| $F$                | force  |
| $h$                | Altitude   |
| $p$                | Roll rate  |
| $q$                | Pitch Rate   |
| $Q$                | Dynamic Pressure   |
| $\mathbb{R}$       | Real Numbers set   |
| $r$                | Yaw rate   |
| $S$                | Wing Area  |
| $t$                | time   |
| $u$                | Longitudinal Velocity  |
| $u_c$              | Control Vector   |
| $v$                | velocity   |
| $x$                | position   |
| $\beta$            | Slip Angle   |
| $\delta_r$         | Roller rate  |
| $\delta_T$         | Throttle Fraction  |
| $\delta_\alpha$    | Aileron rate   |
| $\varepsilon_T$    | Thrust Vector  |
| $\theta$           | Inclination of the Wing tip  |
| $\tau$             | Effectivity of the flap  |
| $\Phi$             | Planning Angle   |
| $\vec{\omega}$     | Angular Speed  |
| $\omega$           | Vertical Speed   |



# Abstract

Urban Air Mobility (UAM) represents a transformative paradigm in transportation, propelled by advancements in Vertical Takeoff and Landing (VTOL) technology. This master's dissertation delves into the intricate dynamics and control aspects of VTOL aircraft, specifically focusing on the transition from hover to forward flight for UAM applications. The research centers on three interconnected goals: optimizing Linear Quadratic Regulator (LQR) controllers, addressing practical implementation challenges, and conducting a simulation-based analysis of controller performance.

The investigation into LQR controllers reveals their potential for fine-tuning control strategies during the critical VTOL transition phase. Achieving enhanced stability, precision, and efficiency, this optimization contributes not only to theoretical control frameworks but also establishes a practical foundation for robust and adaptive control systems in VTOL UAM aircraft.

Exploration of practical implementation challenges provides valuable insights into real-world constraints associated with VTOL transition. Propulsion system dynamics, aerodynamic effects, and sensor limitations are scrutinized, offering a roadmap for integrating advanced control algorithms into operational UAM vehicles.

A rigorous simulation-based analysis evaluates the performance of optimized LQR controllers in dynamic flight environments. Validating their efficacy and providing a platform for sensitivity analysis, this analysis is crucial for anticipating and mitigating challenges in real-world applications.

Reflecting on the implications of this research, the optimized LQR controllers, coupled with a deeper understanding of practical challenges, stand to reshape the landscape of VTOL UAM aircraft. This simulation-based analysis not only validates controllers but serves as a predictive tool for assessing robustness across diverse operational conditions.

Looking ahead, the goals achieved in this dissertation set the stage for continued advancements in UAM. The optimized LQR controllers, informed by practical considerations, provide a foundation for further exploration and adaptation. Future research may extend into lateral flight, application of Gain Scheduling control strategies, experimental validations, real-world testing, and the integration of additional control features to enhance adaptability in dynamic urban environments.

In conclusion, this research contributes significantly to the discourse on urban air mobility. By addressing specific goals and providing actionable insights, it expands the theoretical framework and offers valuable guidance for engineers, researchers, and policymakers involved in the development of VTOL UAM systems. This dissertation represents a pivotal milestone in the pursuit of safe, efficient, and sustainable urban air transportation, laying the groundwork for the seamless transition from hover to forward flight in VTOL aircraft.

## **Key-Words**

VTOL, UAM, Transition Phase, Longitudinal Control, LQR Design



# Resumo Alargado

Nos últimos anos, a evolução da engenharia autônoma, exemplificada pelos avanços em Inteligência Artificial (IA), transformou várias indústrias. O setor aeronáutico testemunhou uma mudança de paradigma com o surgimento de Veículos Aéreos Não Tripulados (VANTs) e o advento de Aeronaves de Mobilidade Aérea Urbana (AMAU). Apesar do rápido progresso, existe uma lacuna crítica na compreensão e implementação de sistemas de controle fiáveis para aeronaves de Descolagem e Aterragem Verticais (VTOL) durante a transição de pairar para voo frontal.

A Mobilidade Aérea Urbana (AMAU) visa a utilização de aeronaves pequenas, alimentadas por eletricidade, para transporte eficiente em áreas urbanas e suburbanas. Este conceito ganhou impulso devido aos avanços tecnológicos, particularmente na propulsão elétrica e sistemas autônomos. Grandes empresas como a UBER e a Airbus estão a investir bastante na AMAU, prevendo um futuro onde as deslocações entre cidades são rápidas, confortáveis e autônomas. Aeronaves VTOL, frequentemente parte da frota AMAU, desempenham um papel fundamental, permitindo descolagens e aterragens sem pistas tradicionais.

Os objetivos principais desta tese são triplos. Em primeiro lugar, visa otimizar os controladores Linear Quadratic Regulator (LQR) do Modo Longitudinal durante a fase crítica de transição de voo pairado para voo frontal em aeronaves VTOL e inserir ainda o conceito de propulsão vetorizada neste controlador. Isso envolve aprimorar os ganhos de controle, considerar diversas configurações de aeronaves e realizar simulações aprofundadas para aplicações no mundo real. Em segundo lugar, a pesquisa aborda desafios práticos de implementação associados aos sistemas de controle VTOL, lidar com incertezas. Por último, a dissertação conduz uma análise baseada em simulação do desempenho do controlador, avaliando vários controladores em diferentes condições ambientais e operacionais.

A revisão do estado da arte em controladores VTOL é explorada, enfatizando a paisagem dinâmica de pesquisa e desenvolvimento. Estratégias de controle, como controladores Proporcional-Integral-Derivativo (PID), Controle Preditivo de Modelo (MPC) e controladores LQR, são discutidas. São destacados controladores personalizados para diferentes configurações VTOL, especialmente a versatilidade dos controladores LQR. Desafios práticos de implementação, incluindo ruído do sensor e incertezas em ambientes operacionais complexos, são reconhecidos, enfatizando a necessidade de melhorias na robustez.

A pesquisa é estruturada de forma sistemática, começando por uma base teórica sólida que estabelece princípios relevantes para aeronaves VTOL e design de controladores. Aprofunda-se nas características e complexidades únicas das aeronaves VTOL, fornecendo uma base para a modelação detalhada. O foco crítico é o Design do Controlador, abrangendo o estado de equilíbrio, linearização, controlabilidade, observabilidade e estabilidade dinâmica. Explora-se a implementação de controladores LQR, e uma análise de regulamentação da Agência Europeia para a Segurança da Aviação (EASA) e da Administração Federal de Aviação (FAA) é incluída.

A dissertação contribui para o avanço do campo de sistemas de controle VTOL, abordando lacunas identificadas. Propõe controladores LQR otimizados para transições mais suaves durante o voo de aeronaves VTOL, oferece soluções práticas para desafios de implementação e conduz uma análise abrangente baseada em simulação do desempenho do controlador. A natureza interligada destas contribuições assegura uma abordagem holística para melhorar os sistemas de controle VTOL, tornando-os mais fiáveis e eficientes em diversos contextos operacionais.

Conclui-se esta dissertação com uma síntese das principais descobertas, enfatizando a sua importância no contexto mais amplo da dinâmica e controle de aeronaves VTOL. Insights sobre potenciais áreas para futuras pesquisas são fornecidos, reconhecendo a natureza dinâmica e evolutiva do campo. A abordagem estruturada garante uma exploração abrangente da

dinâmica e controlo de aeronaves VTOL, oferecendo informações valiosas para investigadores, engenheiros e decisores na indústria da aviação.

Esta pesquisa não é apenas um empreendimento académico, mas um passo crucial para moldar o futuro do voo autónomo. Ao desvendar as complexidades da dinâmica VTOL e aprimorar os sistemas de controlo, a tese contribui para uma nova era na aviação, onde as aeronaves VTOL navegam de forma impecável pelos cenários urbanos com precisão, confiabilidade e eficiência.

**Palavras-Chave**

VTOL, UAM, Fase de Transição, Controlo Longitudinal, Projeto de Controlo LQR





# Contents

|          |  |           |
|----------|--|-----------|
| <b>1</b> | <b>Introduction</b>  | <b>23</b> |
| <b>2</b> | <b>Theoretical Framework</b>   | <b>27</b> |
| 2.1      | Lyapunov Theorem . . . . .   | 27        |
| 2.1.1    | Lipschitz Condition . . . . .  | 27        |
| 2.1.2    | Stability Theorem of Lyapunov . . . . .  | 28        |
| 2.1.3    | LaSalle’s Invariance Theorem . . . . .   | 28        |
| 2.1.4    | Linearization Technique and Lyapunov’s First Method . . . . .  | 28        |
| 2.1.5    | Global Exponential Stability . . . . .   | 30        |
| 2.2      | Zubov’s Method . . . . .   | 30        |
| 2.3      | Krasovskii’s Method . . . . .  | 32        |
| 2.4      | Converse Theorems . . . . .  | 32        |
| 2.5      | Input to State Stability . . . . .   | 32        |
| 2.6      | Feedback Control . . . . .   | 33        |
| 2.6.1    | Hurwitz Criterion . . . . .  | 33        |
| 2.6.2    | Control Problem . . . . .  | 33        |
| 2.6.3    | Stabilization via Linearization . . . . .  | 33        |
| 2.7      | Poincaré-Lyapunov Stability Theorem . . . . .  | 34        |
| <b>3</b> | <b>VTOL and Forward Flight Modeling</b>  | <b>37</b> |
| 3.1      | General Model of Motion Equations . . . . .  | 37        |
| 3.2      | Model Of Equations for Transition Flight . . . . .   | 38        |
| 3.3      | Propeller-Induced Airflow Effects . . . . .  | 39        |
| <b>4</b> | <b>Controller Design</b>   | <b>41</b> |
| 4.1      | Aircraft Specifications . . . . .  | 42        |
| 4.2      | Equilibrium State . . . . .  | 42        |
| 4.2.1    | Longitudinal Flight . . . . .  | 43        |
| 4.2.2    | Lateral-directional Flight . . . . .   | 44        |
| 4.2.3    | Results . . . . .  | 46        |
| 4.3      | Linearization of Longitudinal and Lateral-directional flight models around a reference control state . . . . .                               | 46        |
| 4.3.1    | Longitudinal Flight . . . . .  | 46        |
| 4.3.2    | Lateral-directional Flight . . . . .   | 47        |
| 4.4      | Analysis of the controllability, observability and dynamic stability of the aircraft’s longitudinal and Lateral-directional flight . . . . . | 48        |
| 4.4.1    | Longitudinal Flight . . . . .  | 48        |
| 4.4.2    | Lateral-directional Flight . . . . .   | 49        |
| 4.5      | Analysis of the dynamics of the characteristic movements of this aircraft and its flight qualities . . . . .                                 | 49        |
| 4.5.1    | Longitudinal Flight . . . . .  | 50        |
| 4.5.2    | Lateral-directional Flight . . . . .   | 51        |
| 4.6      | LQR controller projection . . . . .  | 52        |
| 4.6.1    | Stabilization for the origin . . . . .   | 53        |
| 4.7      | Stabilization for outside of the origin . . . . .  | 55        |
| 4.7.1    | Control of pitch angle and speed . . . . .   | 55        |
| 4.7.2    | Analysis of the regulations for VTOL Aircraft from the European and USA Authorities . . . . .  | 58        |
| <b>5</b> | <b>Conclusion</b>  | <b>63</b> |



# List of Figures

|    |   |    |
|----|---|----|
| 1  | Non-linear function example [1] . . . . .   | 29 |
| 2  | Representation of the aircraft and the Earth and Body Axes from [2] . . . . .                               | 37 |
| 3  | Representation of the forces and moments acting on the UAV during transition flights from [2] . . . . .     | 38 |
| 4  | Airflow vectors acting on the UAV from [2] . . . . .  | 39 |
| 5  | Effectivity of the flap vs Ratio of the area of the moving part (Flap) . . . . .                            | 45 |
| 6  | Graphic for the Analysis of the Aircraft Flight Qualities . . . . .   | 51 |
| 7  | Schematic representation of an LQR controller . . . . .   | 54 |
| 8  | Stabilization of speedwith for the Origin after implementing LQR . . . . .                                  | 57 |
| 9  | Stabilization of the pitch angle for the Origin after implementing LQR . . . . .                            | 58 |
| 10 | Stabilization of the speed for outside of the Origin after implementing LQR . . . . .                       | 58 |
| 11 | Stabilization of the Pitch Angle for outside of the Origin after implementing LQR . . . . .                 | 59 |
| 12 | Simulation 2 of Stabilization of the Pitch Angle for outside of the Origin after implementing LQR . . . . . | 59 |
| 13 | Simulation 2 of Stabilization of the Speed for outside of the Origin after implementing LQR . . . . .       | 60 |



# List of Tables

|   |  |    |
|---|--|----|
| 1 | VTOL Aircraft Specifications . . . . .         | 42 |
| 2 | Long Period Levels of Quality . . . . .        | 51 |
| 3 | Short Period Levels of quality . . . . .       | 51 |
| 4 | Roll Quality Categories . . . . .              | 52 |
| 5 | Spiral Mode Quality Categories . . . . .       | 52 |
| 6 | Categories of Quality for Dutch Roll . . . . . | 52 |
| 7 | Chosen $\eta$ values . . . . .                 | 56 |
| 8 | Chosen $\lambda$ values . . . . .              | 56 |



# 1 Introduction

In recent years society has evolved to make engineering more and more autonomous and to give less and less responsibility to the human being, which can be seen for example in the sudden evolution that has happened in relation to Artificial Intelligence. In the Aeronautical market the trend is not different from the usual, hence the high demand for Unmanned Aerial Vehicles (UAV) which in turn is bringing to the market Urban Air Mobility (UAM) aircraft. This market although fairly recent already presents a great development and evolution due to the investment that big name companies have made in this area, such as UBER and Airbus for example. The goal is that in the near future we won't need to be stopped for 1 hour in traffic to get to major cities and we can go from Porto to Lisbon, for example, in a short time, with comfort and autonomy without the need and cost of a pilot. Usually the aircrafts used for this purpose are part of the Vertical Take-off and Landing (VTOL) group so that there is no need for a traditional runway as well.

Urban Air Mobility (UAM) refers to a concept that envisions the use of small, electric-powered aircraft for transportation within urban and suburban areas. This idea has been explored for several decades, but recent advancements in technology, particularly in electric propulsion and autonomous systems, have accelerated its development. These aircrafts are often designed to carry a limited number of passengers, typically between one and six, and can operate either piloted or autonomously. This type of aircraft have the potential to revolutionize urban transportation by offering faster and more efficient alternatives to ground-based travel. Some of the anticipated applications of UAM aircraft today include Air Taxi, Emergency Medical Services, Cargo Delivery, Sightseeing and Tourism. The future of UAM aircraft holds even more potential for transformative transportation solutions such as the Integration with Existing Infrastructure of transports, Sustainability and Noise Reduction, Autonomous Operations, etc.

The concept of UAVs dates back to the early 20th century, with the development of remote-controlled aircraft for military purposes. However, significant advancements occurred in the latter half of the 20th century, driven by advancements in technology and computing capabilities. UAVs have evolved from simple remote-controlled models to sophisticated unmanned aircraft equipped with advanced sensors, communication systems, and autonomous capabilities. They come in various sizes, ranging from small hand-launched drones to large, long-endurance military surveillance aircraft. UAVs have found applications in a wide range of sectors including Military and Defense, Aerial Photography and Videography and Delivery and Logistics. This type of aircraft holds immense potential for future in areas such as UAM, Precision Agriculture, Emergency Response and Humanitarian Aid, etc.

The transition from hover to forward flight in a VTOL aircraft involves a significant change in aerodynamic forces and flight characteristics. The transition Process can be explained through 4 steps:

**1. Takeoff and Hover:** During VTOL mode, the aircraft uses its vertical thrust to take off and hovers in a stationary position. The thrust is directed vertically, balancing the weight of the aircraft and generating lift.

**2. Transition Phase:** Once the aircraft achieves a safe altitude in hover, it initiates the transition to forward flight. This transition involves gradually tilting the aircraft's propulsion system, in this case with the use of the Controlled Thrust Vector, to direct thrust in a horizontal direction.

**3. Forward Flight:** As the thrust is redirected horizontally, the aircraft begins to move forward, transitioning from a vertical to a horizontal flight path. The aircraft's control surfaces, such as elevons or ailerons, are engaged to provide stability and control during forward flight.

**4. Conversion:** During the transition, the aircraft's aerodynamic configuration may change, with elements such as rotor blades or propellers adjusting their pitch or stowing to reduce drag. This conversion optimizes the aircraft's aerodynamic efficiency for forward flight.

There are several key aspects that need to be addressed for UAVs and UAM aircraft to become a reality on a broader scale today, one of them being Safety and Reliability. Advancements in technology, including robust flight control systems that can guarantee a smooth and completely safe transition from vertical to horizontal flight are necessary to build trust in the reliability and safety of these aircraft. One of the obstacles that we intend to overcome in this type of aircraft is also the autonomy of the vehicle, in the sense that a pilot will no longer be necessary, and the entire flight will be done autonomously through the development of ultra-reliable controllers. This project will consist on the research, development and analysis of a Controller that will be able to make a smooth transition from Hover to Horizontal Flight in an UAM with fixed wing using Controlled Thrust Vector. The possibility of autonomous flight will be also investigated so that the transition part for vertical flight can be done without the presence of a pilot, which is still not the case today. Comprehensive testing,

certification processes, and adherence to aviation regulations are crucial to instill confidence in the public and regulatory authorities. This topic is one of the most discussed today and needs a lot of analysis, so it will also be covered and discussed in this article.

### **VTOL Aircraft Control**

Vertical Takeoff and Landing (VTOL) aircraft, encompassing unmanned aerial vehicles (UAVs) and their diverse configurations, have witnessed significant advancements in control systems. The state-of-the-art in VTOL controllers reflects a dynamic landscape of research and development, with a focus on addressing the unique challenges posed by the transition from hover to forward flight.

Recent research has explored a spectrum of advanced control strategies to enhance the performance of VTOL aircraft. Proportional-Integral-Derivative (PID) controllers, Model Predictive Control (MPC), and Linear Quadratic Regulator (LQR) controllers have been at the forefront. The integration of these strategies aims to achieve precise and adaptable control during critical transition phases, considering the diverse aerodynamic and operational characteristics of VTOL platforms.

Acknowledging the diversity in VTOL aircraft designs, studies have emphasized the importance of tailoring control strategies to specific configurations. Tilt-rotor, tilt-wing, and other unique designs present distinct challenges during transition phases. State-of-the-art research recognizes the need for customized controllers that can optimize stability and responsiveness based on the aerodynamic nuances inherent in different VTOL platforms.

Linear Quadratic Regulator (LQR) controllers have emerged as a key focus area within the state-of-the-art landscape. Research has delved into refining LQR-based control strategies, optimizing controller gains, and adapting these controllers to the intricacies of VTOL dynamics. The versatility of LQR controllers in providing stability while allowing for dynamic transitions has positioned them as a promising solution for VTOL aircraft.

Despite significant progress in theoretical models and simulations, the state-of-the-art in VTOL controllers acknowledges the challenges associated with practical implementation. Factors such as sensor noise, external disturbances, and uncertainties in operational environments highlight the need for robustness enhancements to ensure the effectiveness of control systems in real-world scenarios.

The evolving nature of VTOL missions, often in dynamic and unpredictable environments, has spurred interest in adaptive control paradigms. State-of-the-art research recognizes the importance of developing controllers that can adapt to changing conditions, thereby enhancing the overall resilience and performance of VTOL aircraft in response to unforeseen challenges.

In conclusion, the current state-of-the-art in controllers for VTOL aircraft reflects a multidisciplinary approach, encompassing advanced control strategies, tailored configurations, and a focus on practical implementation challenges. As technology continues to evolve, the trajectory of research in this domain aims to bridge existing gaps, providing solutions that balance stability, adaptability, and efficiency in the dynamic realm of VTOL operations.

### **Objectives**

My thesis aims to address three interconnected aspects related to Vertical Takeoff and Landing (VTOL) aircraft, with a focus on optimizing Linear Quadratic Regulator (LQR) controllers during longitudinal flight transitions, tackling practical implementation challenges, and conducting a simulation-based analysis of controller performance.

A critical focus of the dissertation is the Controller Design, which is divided into several crucial elements. The equilibrium state of the VTOL aircraft is defined, laying the groundwork for the subsequent linearization of longitudinal and latero directional flight around a reference control state.

The analysis then extends to evaluating controllability, observability, and dynamic stability based on the linearized models. This includes a meticulous examination of the aircraft's characteristic movements and overall flight qualities. The implementation of Linear Quadratic Regulator (LQR) projection further refines the controller design.

A unique aspect of the research involves an analysis of regulations for VTOL aircraft, incorporating guidelines from both the European Aviation Safety Agency (EASA) and the Federal Aviation Administration (FAA).

The thesis culminates in a comprehensive conclusion that synthesizes key findings, emphasizing their significance in the broader context of VTOL aircraft dynamics and control. The conclusion also provides insights into potential avenues for future research in this dynamic and evolving field.

By intertwining these overarching goals, the dissertation seeks to provide a holistic approach to optimizing LQR controllers for VTOL transitions, ensuring not only theoretical enhancements but also practical implementations that address real-world challenges. The integration of refined control strategies with practical solutions, coupled with a thorough simulation-based analysis, is aimed at

advancing the field of VTOL control systems, ultimately contributing to the development of more reliable and efficient VTOL aircraft.

### **Dissertation Outline**

This dissertation addresses the intricate dynamics and control aspects of Vertical Take-Off and Landing (VTOL) aircraft. The research is organized into key components, beginning with a solid theoretical framework that establishes the foundational principles relevant to VTOL aircraft and controller design and written based on a classic book, [3].

The theoretical framework encompasses a comprehensive exploration of stability analysis methods in control theory. It begins with Lyapunov's stability theorem, elucidating key components such as Lipschitz conditions, LaSalle's invariance theorem, and global exponential stability. The section also introduces Zubov's and Krasovskii's methods, offering alternative approaches to stability assessment. Converse theorems are discussed, addressing conditions for the reversal of stability conclusions. Input to State Stability is presented, emphasizing the system's resilience to external inputs. The segment on feedback control covers the Hurwitz Criterion, general control problems, and stabilization via linearization. The framework culminates with the Dynamic Systems Stability Theorem, likely integrating insights from Poincaré and Lyapunov, providing a robust foundation for analyzing and designing control systems with diverse and dynamic behaviors.

In the second part, "VTOL and Forward Flight Modeling," the focus is on understanding the motion equations governing VTOL aircraft. The first subchapter provides a general model, offering a foundational framework. The second subchapter zooms in on transitional flight, examining the specific equations during the shift from vertical to forward motion. The third subchapter explores the impact of propeller-induced airflow on overall modeling. This chapter is a fundamental resource, setting the stage for deeper analyses of the complex dynamics involved in VTOL and forward flight in subsequent sections.

In the final chapter, "Controller Design," the emphasis is on designing a controller for VTOL aircraft. It begins with aircraft specifications, followed by discussions on equilibrium states, linearization of flight models, and a thorough analysis of controllability and stability. The chapter delves into the characteristic movements and flight qualities of the aircraft, progressing to the design and projection of a Linear Quadratic Regulator (LQR) controller. Specific attention is given to stabilization for both the origin and outside of the origin, particularly focusing on pitch angle and speed control. The chapter concludes with a comprehensive analysis of regulations from European and USA authorities, offering a holistic exploration of the VTOL aircraft controller design process.

Simultaneously, the last part of the dissertation focuses on addressing practical implementation challenges associated with VTOL control systems. This involves a detailed exploration of the hurdles faced in translating theoretical controller designs into robust, real-world applications. The challenges may encompass issues such as dealing with uncertainties that arise in complex real-world environments and overcoming hardware limitations that may impact the performance of the control system. The objective is to propose solutions that improve the robustness and reliability of VTOL control systems in practical scenarios.

In the end of the chapter 4 there is a simulation-based analysis of controller performance. This aims to conduct an extensive evaluation of various controllers under different environmental and operational conditions. This simulation-based analysis serves to provide a comprehensive understanding of how the optimized LQR controllers perform in a range of scenarios, further informing their practical applicability and effectiveness in diverse operational contexts.

This structured approach ensures a thorough exploration of VTOL aircraft dynamics and control, offering valuable insights for researchers, engineers, and policymakers in the aviation industry.

By intertwining these three overarching goals, the thesis seeks to provide a holistic approach to optimizing LQR controllers for VTOL transitions, ensuring not only theoretical enhancements but also practical implementations that address real-world challenges. The integration of refined control strategies with practical solutions, coupled with a thorough simulation-based analysis, is aimed at advancing the field of VTOL control systems, ultimately contributing to the development of more reliable and efficient VTOL aircraft.



## 2 Theoretical Framework

### 2.1 Lyapunov Theorem

When we talk about systems control, we can split it into two big groups: Linear and Non-linear systems. For a system to be linear, it must satisfy the following properties: homogeneity, that is, when the input  $x(t)$  is multiplied by a value, the output  $y(t)$  is also multiplied by this value. If the inputs are  $k \cdot x(t)$ , then the outputs will be  $k \cdot y(t)$  and additivity, which means that if the input is the sum of  $x_1$  and  $x_2$ , the output is  $y_1 + y_2$ .

If it does not satisfy these properties, the system is nonlinear, which happens in the case of the system analyzed in this thesis.

Every aircraft is a non-linear dynamic system like any existing physical system. Today there is still no universal method to study this type of system, however there are a lot of tools which allow us to analyze them like the Lyapunov Stability Theorem which analyzes the domain of attraction of a certain point of equilibrium and its stability through a function  $V$ , Lyapunov's function.

In order to understand this Theorem, some concepts must be known as the Equilibrium state, the Lipschitz Condition, LaSalle's Invariance Principle, Linearization Technique and the First Method of Lyapunov, Global Exponential Stability, Boundedness and Input Output Stability. All the previously mentioned concepts will be explained and I will start by a brief explanation of what is an equilibrium point.

For dynamic systems, stability is the capacity of the system to come back to its equilibrium state and when this happens, we say that the system is in its state of equilibrium or on a point of equilibrium. This point is said to be stable if all the solutions that start at nearby points stay in this same neighborhood. However, defining a stable equilibrium point is not as simple as it seems here, so we'll use Lyapunov's method later on for a more in-depth approach.

#### 2.1.1 Lipschitz Condition

First, let's look at the Lipschitz Condition Theorem:

*A function  $f(x)$  satisfies a Lipschitz condition in the variable  $y$  on a set*

$$D \subset \mathbb{R}^n$$

*if a constant  $L > 0$  exists with:*

$$\|f(x) - f(y)\| \leq L\|x - y\| \quad (1)$$

*whenever  $(x), (y)$  are in  $D$ . With  $L$  as Lipschitz constant.*

Therefore, a function  $f(x)$  Lipschitz is said to be one that is uniformly continuous on any bounded interval. In a mathematic point of view we can say that exists  $\epsilon > 0$  such that for any  $\delta > 0$

$$x, y \in D$$

satisfying

$$\|x - y\| < \delta \quad (2)$$

and

$$\|f(x) - f(y)\| \geq \epsilon \quad (3)$$

A Lipschitz function can have this condition globally if  $L$  does not depend on  $x$  and locally if the Lipschitz constant depends on  $x$ . It is also important to note that only because a function is uniformly continuous does not imply that it is Lipschitz.

Applying this concept to system dynamics, for a system to satisfy the Lipschitz condition it must always change its trajectory gradually, that is, there can never be a drastic change in the system. Normally in engineering a function  $f$  is continued piecewise only. When a function is Lipschitz it basically means that its derivative is bounded. For example the square root of  $x$  is not considered as Lipschitz in the origin because the derivative is approximately infinite. We can also say that there are no exaggerated variations in the function for it to follow this condition. If we pay attention to the mathematical definition and divide the two members of the equation by  $|x-y|$  we can conclude that the magnitude of any change in the function must be less than  $L$ .

### 2.1.2 Stability Theorem of Lyapunov

Considering the following equation  $\dot{x} = f(x)$  and that  $x_e = 0$  is the equilibrium state of the system, that  $x_e \in \mathbb{R}$  and that  $f$  is Locally Lipschitz in  $x_e$ . Let  $V : \mathbb{R}^n \rightarrow \mathbb{R}^+$  be a continuously differentiable function. For the equilibrium state to be stable it must satisfy the following conditions:

1.  $V(x) > 0$  for every  $x \neq x_e, V(x_e) = 0$ , which means it is a positively definite function.
  2.  $\dot{V}(x) = \frac{dV}{dx} f(x) \leq -W(x) \leq 0, \dot{V}(x_e) = 0$ , this means that the Lyapunov function has to be a decreasing function.
  3.  $V(x) \rightarrow \infty$  when  $\|x\| \rightarrow \infty$  (radially bounded).
- For flight dynamics models,  $f$  is locally Lipschitz.

### 2.1.3 LaSalle's Invariance Theorem

Let  $\Omega \subset D$  be a compact set that is positively invariant with respect to  $\dot{x} = f(x)$ . Let  $V : \mathbb{R}^n \rightarrow \mathbb{R}$  be a continuously differentiable, radially bounded, positive definite function such that  $\dot{V}(x) \leq 0$  in  $\Omega$ . Let  $E$  be the set of all points in  $\Omega$  where  $\dot{V}(x_e) = 0$ . Let  $M$  be the largest invariant set in  $E$ . Then every solution starting in  $\Omega$  approaches  $M$  as  $t \rightarrow \infty$ .

- If  $x_e$  be an equilibrium point for  $\dot{x} = f(x)$ . Let  $V : D \rightarrow \mathbb{R}$  be a continuously differentiable positive definite function on a domain  $D$  containing the origin  $x = 0$ , such that  $\dot{V}(x) \leq 0$  in  $D$ . Let  $S = \{x \in \mathbb{R}^n \mid \dot{V}(x) = 0\}$  and suppose that no solution can stay identically in  $S$ , other than trivial solution  $x(t) \equiv 0$ . Then, the origin is asymptotically stable.
- Now let  $x_e$  be an equilibrium point for  $\dot{x} = f(x)$ . Let  $V : D \rightarrow \mathbb{R}$  be a continuously differentiable positive definite function on a domain  $D$  containing the origin  $x = 0$ , such that  $\dot{V}(x) \leq 0$  for all  $x \in \mathbb{R}^n$ . Let  $S = \{x \in \mathbb{R}^n \mid \dot{V}(x) = 0\}$  and suppose that no solution can stay identically in  $S$ , other than trivial solution  $x(t) \equiv 0$ . Then, the origin is globally asymptotically stable.

This principle is a latest method, published in 1960 while Lyapunov Method refers to 1892, to analyze the stability of a dynamic system that quite meets the requirements of Lyapunov. It is important to have in mind, in this part, the definition of a positively invariable set which can be named as the set  $\Omega$  with respect to  $\dot{x} = f(x)$  if  $x(0) \in \Omega \Rightarrow x(t) \in \Omega, \forall t \geq 0$ . So considering that  $\Omega$  is a set positively invariable,  $V$  a continuously differentiable function in  $\Omega$  such that  $\dot{V}(x) \leq 0$  in  $\Omega, E \subset \Omega$  is a set of all the points in  $\Omega$  with  $\dot{V}(x) = 0$  and being  $M$  the biggest positively invariable set in  $E$ . Thus, every solution that starts in  $\Omega$  must approach  $M$  as  $t$  tends to infinite.

The asymptotically stable equilibrium is the positive limiting set of any solution that starts close enough to the equilibrium point.

Comparing with Lyapunov's theorem the most salient difference is that the first condition is not necessarily true for all values of  $x$  but for almost all values of  $x$ . So we can conclude that LaSalle's Theorem less conservative than Lyapunov's Theorem and that is the main reason why the first one is mostly used for Stability Analysis and the second one for Controller Design because it has more requirements for Stability Analysis.

### 2.1.4 Linearization Technique and Lyapunov's First Method

Let's consider now the nonlinear function  $f(x)$  represented below where  $dx$  are the disturbances of the system.

Let  $\dot{x} = f(x, u)$  be a continuously differentiable function that represents a system whose equilibrium state is  $f(x_e, u_e) = 0$  with:

- $$x(t) = x_e(t) + \delta_x(t) \tag{4}$$

- $$u(t) = u_e + \delta_u(t) \tag{5}$$

Let  $\delta_x(t)$  e  $\delta_u(t)$  be disturbances then follows the following equation:

$$\dot{x}(t) = f(x_e + \delta_x(t), u_0 + \delta_u(t)) \tag{6}$$

If we apply the Taylor expansion we get:

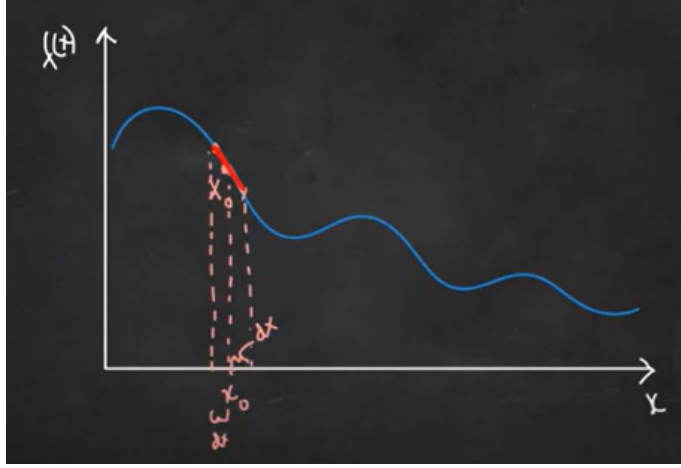


Figure 1: Non-linear function example [1]

$$\begin{aligned} \dot{x}(t) = & f(x_e, u_e) + \frac{\partial}{\partial x} f(x_e, u_e) \delta x + \frac{\partial}{\partial u} f(x_e, u_e) \delta u + \frac{1}{2} \frac{\partial^2}{\partial x^2} f(x_e, u_e) (\delta x)^2 \\ & + \frac{1}{2} \frac{\partial^2}{\partial u^2} f(x_e, u_e) (\delta u)^2 + \dots \end{aligned} \quad (7)$$

Considering that  $h(x_e, u_e, \delta x \delta u) = \frac{1}{2} \frac{\partial^2}{\partial x^2} f(x_e, u_e) (\delta x)^2 + \frac{1}{2} \frac{\partial^2}{\partial u^2} f(x_e, u_e) (\delta u)^2 + \dots$ ,  $\dot{x}$  can be represented by:

$$\dot{x}(t) = f(x_e, u_e) + \frac{\partial}{\partial x} f(x_e, u_e) \delta x + \frac{\partial}{\partial u} f(x_e, u_e) \delta u + h(x_e, u_e, \delta x \delta u) \quad (8)$$

With

$$\frac{\partial f}{\partial x} = \begin{bmatrix} \frac{\partial f_1}{\partial x_1} & \frac{\partial f_1}{\partial x_2} & \dots & \frac{\partial f_1}{\partial x_n} \\ \frac{\partial f_2}{\partial x_1} & \dots & \dots & \frac{\partial f_2}{\partial x_n} \\ \vdots & \dots & \dots & \vdots \\ \frac{\partial f_n}{\partial x_1} & \dots & \dots & \frac{\partial f_n}{\partial x_n} \end{bmatrix}_{x_e, u_e} \quad (9)$$

$$\frac{\partial f}{\partial u} = \begin{bmatrix} \frac{\partial f_1}{\partial u_1} & \frac{\partial f_1}{\partial u_2} & \dots & \frac{\partial f_1}{\partial u_n} \\ \frac{\partial f_2}{\partial u_1} & \dots & \dots & \frac{\partial f_2}{\partial u_n} \\ \vdots & \dots & \dots & \vdots \\ \frac{\partial f_n}{\partial u_1} & \dots & \dots & \frac{\partial f_n}{\partial u_n} \end{bmatrix}_{x_e, u_e} \quad (10)$$

But in a small region above  $x_e$  and for small changes in the input, the behavior of the system can be approximated through the local linearization equation given by:

$$\dot{x}(t) = \frac{\partial}{\partial x} f(x_e, u_e) \delta x + \frac{\partial}{\partial u} f(x_e, u_e) \delta u, \text{ with } \delta x \text{ e } \delta u \text{ as disturbances.} \quad (11)$$

As it is a set of systems of linear equations, which do not vary in time, all available methods for the analysis of linear systems can now be used to analyze the stability of this system. For example, consider the following system:

$$\begin{cases} \dot{x}_1 = -x_1 + x_1 x_2 \\ \dot{x}_2 = -x_2 \end{cases}$$

$x_1 = n$  where  $n = 0, 1, 2$ , etc ..., starting by  $n = 0$  we get the equilibrium point  $(0, 0)$ .

Let us consider then  $f_1(x_1, x_2) = -x_1 + x_1 x_2$  and  $f_2(x_1, x_2) = -x_2$  and their derivatives respectively:

$$\begin{cases} \frac{\partial f_1}{\partial x_1} = -1 + x_2 \\ \frac{\partial f_1}{\partial x_2} = x_1 \\ \frac{\partial f_2}{\partial x_1} = 0 \\ \frac{\partial f_2}{\partial x_2} = -1 \end{cases}$$

This way for the equilibrium point  $(x_1, x_2) = (0, 0)$  we have:

$$\begin{cases} \frac{\partial f_1}{\partial x_1} = -1 \\ \frac{\partial f_1}{\partial x_2} = 0 \\ \frac{\partial f_2}{\partial x_1} = 0 \\ \frac{\partial f_2}{\partial x_2} = -1 \end{cases}$$

So the linearized system of equations is

$$\delta \dot{x} = \begin{bmatrix} -1 & 0 \\ 0 & -1 \end{bmatrix} \delta x \quad (12)$$

To determine the location of the eigenvalues for the linearized system of equations, the following equation is used:

$|\lambda I - A| = 0$ , being  $A$  the matrix which represents the linearized system of equations

$$\left| \begin{bmatrix} \lambda & 0 \\ 0 & \lambda \end{bmatrix} - \begin{bmatrix} -1 & 0 \\ 0 & -1 \end{bmatrix} \right| = 0 \Leftrightarrow \left| \begin{bmatrix} \lambda + 1 & 0 \\ 0 & \lambda + 1 \end{bmatrix} \right| = 0 \Leftrightarrow (\lambda + 1)^2 = 0 \Leftrightarrow \lambda = -1$$

The first Lyapunov Method is mostly used for autonomous systems and applies based on the following equation  $\dot{X} = f(x)$ .

Let  $\delta \dot{X} = \frac{\partial f(x_e)}{\partial x} \delta x + h(x_e, \delta x)$ , where  $h(x_e, \delta x)$  represents the higher order terms, be the equation of the perturbed system from an equilibrium point  $x_e$ . If  $\lim_{\|\delta x\| \rightarrow 0} \frac{h(x_e, \delta x)}{\|\delta x\|} = 0$ , then:

1. If the linearized system  $dX = df(x_e) dx$  has only eigenvalues with negative real parts,  $x_e$  is asymptotically stable
2. If the linearized system has 1 or more eigenvalues with positive real parts,  $x_e$  is unstable.
3. If the linearized system has 1 or more eigenvalues with 0 real parts and the remaining eigenvalues have negative real parts, the stability of  $x_e$  is not accurate just studying the linear system, even the stability "in the small".

As  $\lambda = -1$  we conclude that this system is asymptotically stable.

### 2.1.5 Global Exponential Stability

Let  $x_e = 0$  be the equilibrium point of  $\dot{x} = f(x)$ ,  $x(0) = x_0$  and assuming that  $f(x)$  is Locally Lipschitz, that is, if  $X$  is a compact metric space, then  $f$  is locally Lipschitz if and only if it is a compact function on any subset of  $X$ .  $V : \mathbb{R}^n \rightarrow \mathbb{R}^+$  is a continuously differentiable and radially unbounded function that satisfies the following conditions:

$$V(x) = x^T P x > 0, \forall x \neq 0$$

$$\dot{V}(x) = -x^T Q x < 0, \forall x \neq 0$$

With constant matrices, this is,  $P = P^T$  e  $Q = Q^T > 0$  (that is, the eigenvalues of  $Q$  are all positive) then  $x_e$  is globally and exponentially stable.

So we can conclude that basically Global Stability means that the system is stable in the neighborhood of any equilibrium state.

## 2.2 Zubov's Method

Zubov's method enables to describe the largest attraction domain of a system corresponding to an equilibrium state.

If  $\dot{x} = f(x), t \in \mathbb{R}$  is an ordinary differential equation in  $\mathbb{R}^n$  with  $f(0) = 0$ , a set  $A$  containing 0 in its interior is the domain of stability of 0 if and only if there exists continuous functions  $v, h$  such that:

- $v(0) = h(0) = 0, 0 < v(x) < 1$  for  $x \in A \setminus \{0\}$  and  $h > 0$  on  $\mathbb{R}^n \setminus \{0\}$
- For every  $\gamma_2 > 0$  there exists  $\gamma_1 > 0, \alpha_1 > 0$  such that  $v(x) > \gamma_1$  and  $h(x) > \alpha_1$  if  $\|x\| > \gamma_2$
- $\lim_{n \rightarrow \infty} v(x_n) = 1$
- 

$$\nabla v(x) \cdot f(x) = -h(x)[1 - v(x)]\sqrt{1 + \|f(x)\|^2} \quad (13)$$

When we talk about domain of stability it means every  $x$  in that domain that will be attracted by the equilibrium state and we can also call it domain of influence because it is every  $x$  which is influenced by the equilibrium state. Zubov's Theorem is only useful for non-linear systems because for the linear systems the domain of stability is the full state space (for a stable system)

As we see, according to the Russian mathematician V.I. Zubov, a Lyapunov function can be found for those systems wick the trivial solution is asymptotically stable, with the solution of one partial differential equation and if such equation has a bounded solution, then the Lyapunov function is said to be unique and will allow us to find the exact domain of asymptotic stability. Zubov's method is extremely important to find the boundedness of the Lyapunov function wick follows the equation  $v(x) = 1$ .

Let us consider the next system example:

$$\dot{x}_1 = -x_1 + 2x_1^2x_2 \quad (14)$$

$$\dot{x}_2 = -x_2 \quad (15)$$

First we choose a function, here called  $\varphi(x)$  :

$$\varphi(x) = h(x)\sqrt{1 + \|f(x)\|^2} = x_1^2 + x_2^2 \quad (16)$$

This way, the partial differential equation is

$$\frac{\partial v}{\partial x_1} (-x_1 + 2x_1^2x_2) + \frac{\partial v}{\partial x_2} (-x_2) = -(x_1^2 + x_2^2)(1 - v) \quad (17)$$

This equation can be solved if we find a solution for the associated system of ordinary differential equations:

$$\frac{dx_1}{f_1(x)} = \frac{dx_2}{f_2(x)} = \frac{dv}{-\varphi(x)(1/v)} \quad (18)$$

In this case the  $v$  function founded is

$$v(x) = 1 - \exp\left(-\frac{x^2}{2} - \frac{x_1^2}{2(1 - x_1x_2)}\right) \quad (19)$$

As we know the boundedness is given by  $v(x) = 1$

When we have  $xy = 1$ , the condition up is satisfied, so this curve defines the exact boundedness of the asymptotic stability domain of the system.

We can use another Lyapunov function, doing the substitution

$$v = -\ln(1 - v) \quad (20)$$

If we derive both terms, we have:

$$\frac{dv}{dt} = \frac{1}{1 - v} \cdot \frac{dv}{dt} \quad (21)$$

Now replacing in the differential equation

$$\frac{\partial v}{\partial x_1} f_1 + \frac{\partial v}{\partial x_2} f_2 = -\varphi(x)$$

We can conclude that we have now a new condition which defines the boundedness of exact domain of asymptotic stability:  $v \rightarrow \infty$  when  $\|x\| \rightarrow \infty$ .

So we have

$$\frac{\partial v}{\partial x_1} (-x_1 + 2x_1^2 x_2) + \frac{\partial v}{\partial x_2} (-x_2) = -(x_1^2 + x_2^2) \quad (22)$$

Which solution is given by

$$v(x) = \frac{x_2^2}{2} + \frac{x_1^2}{2(1 - x_1 x_2)} \quad (23)$$

So with the boundedness condition changed it takes us to  $xy = 1$ .

## 2.3 Krasovskii's Method

Theorem: Let us consider the autonomous equation  $\dot{x}(t) = f(x(t))$ ,  $x : \mathbb{R} \rightarrow \mathbb{R}^n$ , where  $f : \mathbb{R} \rightarrow \mathbb{R}^n$  is of the class  $\mathcal{C}^1(\mathbb{R}^n)$  and such that  $f(0) = 0$ . Let's suppose that exists a function  $V : \mathbb{R}^n \rightarrow [0, \infty[$ ,  $V \in \mathcal{C}^1(\mathbb{R}^n)$  such that:

a.  $V(x_0) > 0$  if  $x_0 \neq 0$ ,  $V(0) = 0$ , sendo  $x_0 : \mathbb{R} \rightarrow \mathbb{R}^n$ .

b.  $V(x_0) \rightarrow \infty$  for  $|x_0| \rightarrow \infty$

c. If  $x(t)$  is any solution other than the trivial one and  $\dot{V}(t) = V(x(t))$  and  $\frac{dV}{dt}(t) < 0 \forall t$

Then, the trivial solution is stable. Instead of c) we can also verify the following condition:

$$c') \frac{d\dot{V}}{dt}(t) = \left\langle \frac{dV}{dx_0}(x(t)), f(x(t)) \right\rangle \leq 0 \quad (24)$$

In the set  $M = \left\{ x_0 \in \mathbb{R}^n : \left\langle \frac{dV}{dx_0}(x_0), f(x_0) \right\rangle = 0 \right\}$  such that no solution  $x(t)$  different from the trivial one is verified.  $\{x(t) : t \geq t_0\} \subset M$  for none  $t_0$ , so the conclusion is valid. This theorem is due to Krasovskii [1952] and the last part is a complement due to LaSalle [1961]. As we can see Krasovskii, basically, defines the Lyapunov function and after that brings a result about asymptotic stability. We can also notice that the theorem concerns about autonomous equations.

## 2.4 Converse Theorems

According to the converse theorems if the system is stable and the Jacobian matrix of  $f$  in  $x_0$  is bounded, which implies that the norm of this matrix is less than a certain value independent of  $x$ , that is, the maximum norm is independent of  $x$ , then there is a Lyapunov function  $V$  for the system  $\dot{x} = f(x)$ .

## 2.5 Input to State Stability

Let us consider a system whose dynamics follows the equation  $\dot{x} = f(x, u)$  and the output variables which are on the area of interest for the application in question can be represented by  $y = h(x)$

In the area of Systems Control, stability usually can be approached in two different ways: Input to State or Input/Output. Basically the input to state stability analyzes if with the input  $u$ , the state  $x$  is stable and in the other hand input/output stability will verify if with the input  $u$ , the output variables are stable or not.

The input/output approach is mostly used in the robustness analysis of linear systems with nonlinear feedback and mild nonlinear uncertainties. For the present system we must focus on nonlinear control systems so next I will present the definition of Input to State Stability, which is the one who fits better this type of system.

The system  $\dot{x} = f(t, x, u)$  is said to be input-to-state stable if there exist a class  $\mathcal{KL}$  function  $\beta$  and a class  $\mathcal{K}$  function  $\gamma$  such that for any initial state  $x(t_0)$  and any bounded input  $u(t)$ , the solution  $x(t)$  exists for all  $t \geq t_0$  and satisfies:

$$\|x(t)\| \leq \beta(\|x(t_0)\|, t - t_0) + \gamma(\|u\|_\infty) \quad (25)$$

## 2.6 Feedback Control

In this part we will get into the tools used in non-linear control. In the beginning I will specify the control problem that is being analysed as there are several control tasks that require the use of feedback.

### 2.6.1 Hurwitz Criterion

According to this criterion, any system can be stable if and only if all the roots in the first column have the same sign or if there is a sign change then the number of sign changes in the first column is equal to the number of roots with positive real parts.

### 2.6.2 Control Problem

First of all, there are many formulations of the control problem that can depend on the design purpose. For stabilization, tracking and disturbance rejection or attenuation we find a number of control problems and for which problem we should have a state feedback version where the output vector can be measured.

In our case the feedback stabilization problem is one of the simplest because the system can be described as linear and time invariant:

$$\dot{x} = Ax + Bu \quad (26)$$

$$y = Cx + Du \quad (27)$$

In our case the state feedback control  $u = -Kx$  preserves linearity of the open-loop system and the origin of the closed-loop system  $\dot{x} = (A - BK)x$  is asymptotically stable if and only if the matrix  $A - BK$  is Hurwitz. This way the state feedback stabilization problem reduces to assign the eigenvalues of  $A - BK$  in the open left-half complex plane. According with linear control theory the eigen values of  $A - BK$  can be arbitrarily assigned. If some values of  $A$ , for example, are not controllable, the stabilization is still possible. For this specific case the pair  $(A, B)$  is called stabilizable an the uncontrollable (open-loop) eigenvalues of  $A$  will be (closed-loop) eigenvalues of  $A - BK$ . If the only thing we can measure is the output  $y$ , we can still use dynamic compensation like the observed-based controller:

$$u = -K\hat{x} \quad (28)$$

$$\dot{x} = A\hat{x} + Bu + H(y - C\hat{x} - Du) \quad (29)$$

to stabilize the system.

The feedback gain,  $K$ , is designed like in state-feedback, such that  $A - BK$  is Hurwitz when the observer gain is designed such that  $A - HC$  is Hurwitz. The closed-loop eigenvalues will consist of the eigenvalues  $A - BK$  and the eigenvalues of  $A - HC$ . The stabilization of  $A - HC$  is connected to the stabilization of  $A - BK$  and requires observability of the pair  $(A, C)$

### 2.6.3 Stabilization via Linearization

To get the stabilization via Linearization we should start by considering the stabilization problem first with the state feedback control and then presenting output feedback. Let us consider the system:

$$\dot{x} = f(x, u) \quad (30)$$

$$\text{where, } A = \left. \frac{\partial f}{\partial x}(x, u) \right|_{x=0, u=0}; B = \left. \frac{\partial f}{\partial u}(x, u) \right|_{x=0, u=0}$$

Assuming that the pair  $(A, B)$  is controllable or at least stabilizable, we can design a matrix  $K$  to assign the eigenvalues of  $A - BK$  to desired location in the open left-half complex plane. Now if we apply the linear state feedback control  $u = -Kx$  to the nonlinear system we get the following closed-loop system:

$$\dot{x} = f(x, -Kx) \quad (31)$$

We can see clearly that the origin is an equilibrium point of the closed loop system, which linearization about the origin  $x = 0$  is given by:

$$\dot{x} = \left[ \frac{\partial f}{\partial x}(x, -Kx) + \frac{\partial f}{\partial u}(x, -Kx)(-K) \right]_{x=0} \quad (32)$$

$$x = (A - BK)x \quad (33)$$

## 2.7 Poincaré-Lyapunov Stability Theorem

We have the system:

$$\dot{x}(t) = f(x(t)), \text{ or } \dot{x} = f(x) \quad (34)$$

with  $S(x_0, t_0, t)$  the solution of the differential equation starting at  $x_0 = x(t_0)$ .

**Equilibrium point:** a point  $x^* \in \mathbb{R}^n$  is called the equilibrium point for the system if  $f(x^*) = 0$ .

**Stability:** The system is said to be stable in the Lyapunov sense around the equilibrium point if  $\forall \varepsilon > 0, \exists \eta > 0$  such that for any  $x_0$  satisfying  $\|x_0 - x^*\| \leq \eta$ , there is  $\|S(x_0, t_0, t) - x^*\| \leq \varepsilon$  for any  $t \geq t_0$ .

**Asymptotic stability:** The system is asymptotically stable in the Lyapunov sense around the equilibrium point if it is stable and if the solution of the system converges to the  $x^*$  equilibrium in the long run.

The asymptotic stability ensures that the system returns completely to equilibrium sooner or later, simple stability ensures that the system stays in the vicinity of equilibrium without necessarily reaching it. Thus, asymptotic stability implies simple stability.

$V : \mathbb{R}^n \rightarrow \mathbb{R}$  is a function of scalar values:

$V$  is positive definite if  $\forall x \neq 0, V(x) > 0$ , and  $V(x) = 0$  for  $x = 0$ .

$V$  is semipositive definit if  $\forall x \neq 0, V(x) \geq 0$ , and  $V(x) = 0$  for  $x = 0$ .

$V$  is negative definite if  $\forall x \neq 0, V(x) < 0$ , and  $V(x) = 0$  for  $x = 0$ .

$V$  is seminegative definit if  $\forall x \neq 0, V(x) \leq 0$ , and  $V(x) = 0$  for  $x = 0$ .

**Theorem:**

We consider the following differential equation in  $\mathbb{R}^n$  :

$$\begin{cases} \dot{x} = Ax + B(t)x + f(x) \\ x(t_0) = x_0 \end{cases}$$

It is assumed that  $A$  is a constant matrix whose eigenvalues have negative real parts, and that  $B(t)$  is a continuous matrix in each  $t \in \mathbb{R}^n$  with the following property:

$$\lim_{t \rightarrow +\infty} \|B(t)\| = 0$$

and that the function  $f(x)$  is continuous at each  $t \in \mathbb{R}^n$  and Lipschitz in  $x$  in the neighborhood of  $x_e = 0$  and with:

$$\lim_{|x| \rightarrow 0} \frac{\|f(x)\|}{\|x\|} = 0$$

Thus, there are positive constants  $C, t_0, \delta, \mu$  such that:

$$(\|x_0\| \leq \delta) \Rightarrow \left( \|S(x_0, t_0, t)\| \leq C \|x_0\| e^{-\mu(t-t_0)} \right), t \geq t_0$$

The equilibrium state  $x_e = 0$  is stable and convergence to this is exponential from any initial conditions in the neighborhood of  $x$ . It is important to note that the above theorem requires the determination of all the eigenvalues of the system. Most of the time, this is a complex calculation because the matrix  $A$  tends to be high-dimensional. So, in practice we use the theorem below to analyze the linear systems modeled by the following equation, where  $\bar{x} = x - x_e$  :

$$\dot{\bar{x}} = A\bar{x} \quad (35)$$

We can conclude that this equation is the one of the linearized model with  $\bar{u} = 0$ , when there are no disturbances in the control, and the matrix  $C$  is the identity matrix. Thus it will be explained in the chapter 4. Controller Design will be based on the linearized model, therefore the Poincare Lyapunov theorem is of paramount interest in guaranting that the controller design for that linearized model applies as well to the original non-linear model.



### 3 VTOL and Forward Flight Modeling

In this part of the paper, following lessons learned with [4] I will describe a complete 6-degree-of-freedom nonlinear mathematical model of a tiltrotor unmanned aerial vehicle (UAV). As the name of my thesis suggests this model is a specific one which focus on the transition from hover to forward flight and vice-versa. While designing the control system I took into account the aerodynamic effect of propeller-induced airstream which is a function of cruise speed, tilt angle and angle of attack. The cross-section area and output velocity of the propeller-induced airstream are calculated with momentum theory.

The target at this point is the deriving of the 6-degree-of-freedom nonlinear mathematical model of the UAV which includes 3 phases: hover, transition, and cruise flight.

#### 3.1 General Model of Motion Equations

Usually to find the dynamic equations of flight we use Newton’s second law which sums up all the external forces acting on a body and equals it to the time derivate of its momentum with respect to the inertial space, as presented in the mathematical form on the next equation:

$$m \left[ \frac{d\vec{V}}{dt} + \vec{\omega} \times \vec{V} \right] = \sum_i \vec{F}_i \quad (36)$$

Regarding the total moment on a body and according with Newton’s second law of Motion, it is defined as the time derivate of moment of momentum (angular momentum) with respect to the inertial space as you can see in the next equation:

$$\sum_i M_i = \frac{d\vec{C}}{dt} + \vec{\omega} \times \vec{C} \quad (37)$$

Assuming that (a) the XZ plane of the UAV is the s is the symmetry plane, (b) the mass of the aircraft doesn’t change, (c) the UAV is a rigid body, (d) Earth is considered as the inertial reference, (e) following the axis system shown in figure 2.

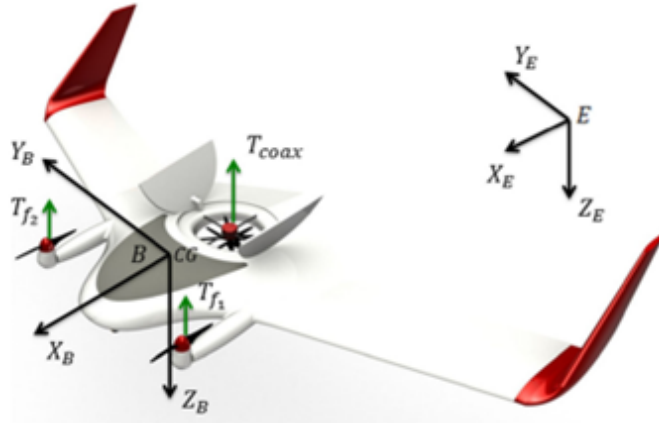


Figure 2: Representation of the aircraft and the Earth and Body Axes from [2]

Using now the assumptions mentioned before together with the the Newton’s second law, we obtain the following equations for the flight dynamics, deriving the equations of force and moment:

$$\dot{u} = -\frac{QS}{m} [C_D \cos \cos(\alpha) \cos \cos(\beta) + C_y \cos \cos(\alpha) \sin(\beta) - C_L \sin(\alpha)] + \frac{T \cos(\epsilon_T)}{m} - g \sin(\theta) - qw + rv \quad (38)$$

$$\dot{v} = -\frac{QS}{m} [C_D \sin(\beta) - C_y \cos \cos(\beta) + g \cos(\theta) \sin(\phi)] - ru + pw \quad (39)$$

$$\dot{w} = -\frac{QS}{m} [C_D \sin(\alpha) \cos \cos(\beta) + C_y \sin(\alpha) \sin(\beta) + C_L \cos \cos(\alpha) + g \cos(\alpha) \cos \cos(\phi)] - pv + qu - \frac{T_c}{m} \quad (40)$$

Where  $T_C$  is the Traction for VTOL and  $T = \delta_T \cdot T_{\max}(V, h)$ , that is,

$$\dot{T} = \frac{1}{\tau} (\delta_T \cdot T_{\max}(V, h) - T) \quad (41)$$

The attitude angles equations are transformed from the Earth axis system for the UAV body axis system through a transformation of the R matrix:

$$[P \ Q \ R] = R[\dot{\phi} \ \dot{\theta} \ \dot{\psi}] \quad (42)$$

With  $[\dot{\phi} \ \dot{\theta} \ \dot{\psi}]$  as the Euler angles

After the deduction we have the final results for the attitude dynamics angles:

$$\dot{\phi} = p + (q \sin \phi + r \cos \phi) \tan \theta \quad (43)$$

$$\dot{\theta} = q \cos \phi - r \sin \phi \quad (44)$$

$$\dot{\psi} = \frac{q \sin \phi + r \cos \phi}{\cos \theta} \quad (45)$$

### 3.2 Model Of Equations for Transition Flight

This part of the flight is the most important to study and also the most complex because it is the moment when the aircraft changes from hover to forward flight. With the smallest change on the tilt angle of the propellers, the force and moment acting on the UAV change so in this phase they are changing continuously since the tilt rotor is moving all the time.

Before going on the mathematical part of the problem, I will exemplify with a picture which are the geometric dimensions, thrust and drag forces that act on the airframe:

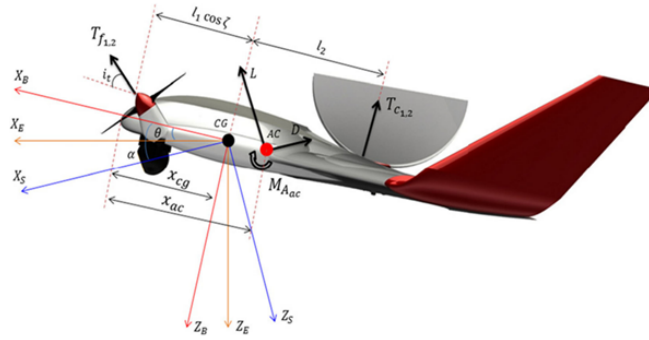


Figure 3: Representation of the forces and moments acting on the UAV during transition flights from [2]

During the hover regime there is no aerodynamic force or moment acting on the aircraft body because there is no forward airspeed but when the motors start to rotate about the tilting axis, it starts to be created an horizontal force proportional to the tilting angle. In that moment Aerodynamic moment lift force, drag force and pitching moment start to affect the UAV.

Now, based on the forces shown in the previous figure, we can write again the maneuvering rate equations for this phase:

$$\dot{p} = \frac{1}{I_x I_z - I_{zx}^2} [I_z (Q S b c_l) + (I_y - I_z) q r] + I_{xz} (Q S b C_n + (I_x - I_y + I_z) p q - I_{xz} q r) \quad (46)$$

$$\dot{q} = \frac{1}{I_y} [Q S c C_m + I_{xz} (r^2 - p^2) + (I_z - I_x) r p - T_c l_2], l_2 \text{ is the distance from } T_c \text{ to g.c.} \quad (47)$$

$$\dot{r} = \frac{1}{I_x I_z - I_{xz}^2} [I_x (Q S b C_n + (I_x - I_y) p q) + I_x (Q S B C_l) + (I_y - I_x - I_z) q r + I_{zx} p q], // \quad (48)$$

where  $Q = 0,5\rho V^2$  and  $b$  is the wingspan.

### 3.3 Propeller-Induced Airflow Effects

Propeller-induced airflow effects refer to the changes in the airflow around an aircraft caused by the rotation of the propeller. As the propeller blades rotate, they create a region of low pressure in front of them and a region of high pressure behind them. These pressure changes cause air to flow around the propeller blades, which can have several effects on the aircraft, such as:

- Thrust: The most obvious effect of the propeller-induced airflow is that it generates thrust, which propels the aircraft forward.
- Slipstream: The high-velocity air behind the propeller, known as the slipstream, can affect the airflow over the wings, tail, and other surfaces of the aircraft. This can increase the lift and drag on these surfaces, as well as affect their stability and control.
- Torque and P-factor: The rotation of the propeller also creates torque, which can cause the aircraft to roll or yaw. Additionally, the propeller's asymmetric shape can create a phenomenon called P-factor, where the aircraft tends to yaw to one side due to the propeller's rotation.
- Engine cooling: The airflow around the propeller can also help to cool the engine by providing a flow of fresh, cool air.

Propeller-induced airflow effects can have a significant impact on VTOL (Vertical Takeoff and Landing) aircraft. Unlike fixed-engine aircraft, VTOL aircraft rely on their propulsion systems to generate lift and control their altitude and direction of flight. As such, any changes in the airflow around the aircraft, such as those caused by propeller rotation, can have a significant impact on the aircraft's stability, control, and performance.

One of the main effects of propeller-induced airflow on VTOL aircraft is the interaction between the propeller's slipstream and the aircraft's lifting surfaces. The high-velocity air in the slipstream can affect the lift and drag on the aircraft's wings, rotors, or other lifting surfaces, which can make it more difficult to control the aircraft. Additionally, the asymmetric shape of the propeller can create yawing moments that can affect the aircraft's stability and control.

Another effect of propeller-induced airflow on VTOL aircraft is the need for precise control of the propeller's thrust vector. In a VTOL aircraft, the direction of the propeller's thrust is critical for controlling the aircraft's altitude and direction of flight. Any changes in the direction of the thrust caused by the propeller's rotation or other factors can make it more difficult to control the aircraft.



Figure 4: Airflow vectors acting on the UAV from [2]



## 4 Controller Design

The transition from hover to forward flight for a VTOL aircraft with fixed wing and controlled by Thrust Vector is considered as a critical phase of flight which requires a careful planning and execution. This is mainly due to the fact that the aircraft needs to maintain stability when changing from vertical to horizontal flight.

This process will follow [4] and usually begins with the aircraft in a vertical hover position, where the thrust vector is pointed down. This is followed by a phase where the thrust vector begins to move forward while simultaneously increasing the forward airspeed of the aircraft, lowering the nose of the aircraft, which causes a gradual transition to horizontal flight.

As the airspeed increases, the lift created by the fixed wing begins to override the lift created by the thrust vector. This requires careful variation of the wing angle of attack to prevent stalling.

To design the Controller we will start by locating an equilibrium state about which we can analyze the stability and Control of this UAV in specific once we have the Specifications. With the equilibrium state found we can proceed to the Linearization of Lateral-directional and Longitudinal Flight around that reference control state. After that we proceed with the analysis of the controllability, observability and dynamic stability of the aircraft as well as the analysis of the characteristic movements and its flight qualities that are for longitudinal flight the short and the long period and for the Lateral-directional Flight are Roll, Dutch Roll and Pitch. Based in all of this analysis we can finally Project the LQR Controller based in all the results obtained before. To close this chapter I will also make a summarized analysis of the Regulations for VTOL Aircrafts from EASA and FAA.

## 4.1 Aircraft Specifications

| Specification [unit]   | Symbol          | Value                           |
|--|-----------------|---------------------------------|
| Wingspan [m]   | b               | 10,692                          |
| Mass [kg]  | m               | 448                             |
| Wing Area [m <sup>2</sup> ]  | S               | 10.691                          |
| Maximum Traction [N]   | $T_{\max}$      | 5199                            |
| Acceleration of gravity [m/s <sup>2</sup> ]  | g               | 9,807                           |
| Medium chord [m]   | $\underline{2}$ | 2                               |
| Derivative of the coefficient of pitching moment with angle of attack rate                       | $C_m$           | $-0,0002 \cdot \alpha + 0,0038$ |
| Moment of Inertia on the plane $xx$ [ kg · m <sup>2</sup> ]                                      | $I_{xx}$        | 494,001                         |
| Moment of Inertia on the plane $zz$ [ kg · m <sup>2</sup> ]                                      | $I_{zz}$        | 16403,76                        |
| Moment of Inertia on the plane $xz$ [ kg · m <sup>2</sup> ]                                      | $I_{xz}$        | 16194,18                        |
| Moment of Inertia on the plane $yy$ [ kg · m <sup>2</sup> ]                                      | $I_{yy}$        | 40,304                          |
| Distance between the aerodynamic center of the horizontal tail and the c.g. of the airplane [cm] | $l_H$           | 368,07                          |
| Position of the aerodynamic center of the aircraft in the $x$ axis [cm]                          | $x_{ac}$        | 368,07                          |
| Position of the center of the aircraft in the $x$ axis [cm]                                      | $x_{cg}$        | 346,07                          |
| Wingspan [m]   | b               | 10,692                          |
| Derivative of the coefficient of pitching moment with angle of attack rate                       | $C_m$           | $-0,0002 \cdot \alpha + 0,0038$ |

Table 1: VTOL Aircraft Specifications

## 4.2 Equilibrium State

To reach the state of equilibrium, it is necessary to use universally known equations as is the case with Newton's second Law (a)(b) and the Flight Dynamics Models (c). In addition, at this stage some assumptions will be made as well as some calculations, based on [5] to find all the values that we need to discover the equilibrium point for this aircraft. Starting from the Flight Dynamics Models:

$$\dot{u} = -\frac{QS}{m} [C_D \cos \cos(\alpha) \cos \cos(\beta) + C_y \cos \cos(\alpha) \sin(\beta) - C_L \sin(\alpha)] + \frac{T \cos(\varepsilon_T)}{m} - g \sin(\theta) - qw + rv \quad (49)$$

$$\dot{v} = -\frac{QS}{m} [C_D \sin(\beta) - C_y \cos \cos(\beta) + g \cos(\theta) \sin(\phi)] - ru + pw \quad (50)$$

$$\dot{w} = -\frac{QS}{m} [C_D \sin(\alpha) \cos \cos(\beta) + C_y \sin(\alpha) \sin(\beta) + C_L \cos \cos(\alpha) + g \cos(\alpha) \cos \cos(\phi)] - pv + qu - \frac{T_c}{m} \quad (51)$$

Considering the symmetry of the vehicle we can now apply these equations to the specific cases of Longitudinal and Lateral-directional flight which allows us to analyze the flight dynamics of an aircraft separately and in more detail.

## 4.2.1 Longitudinal Flight

An aircraft that is longitudinally stable is stable with respect to disturbances around the lateral axis of an aircraft, i.e. disturbances involving pitching and the variation of longitudinal and normal speeds. For longitudinal flight there are no disturbances about the vertical plane, yaw does not vary and the following variables can be neglected:  $v, \Phi, p, r, \delta\alpha$  and  $\delta r$ . Therefore we can describe this type of flight by the following equations:

•

$$\dot{u} = \frac{1}{m} \cdot \left( 0,5 \cdot \rho(h) \cdot S \cdot \frac{u^2}{\cos^2(\alpha)} \right) \cdot (CL \cdot \sin(\alpha) - CD \cdot \cos(\alpha) + \delta T \cdot Tmax \cdot \cos(\varepsilon t)) - g \cdot \sin(\theta) - q \cdot u \cdot \tan(\alpha) \quad (52)$$

•

$$\dot{\alpha} = q + \frac{g \cdot \cos(\alpha)}{u} \cdot \cos(\theta - \alpha) - \frac{\cos(\alpha)}{m \cdot u} \cdot (L - \delta t \cdot Tmax \cdot \sin(\varepsilon t) \cdot \cos(\alpha) + \delta t \cdot Tmax \cdot \cos(\varepsilon t) \cdot \sin(\alpha)) \quad (53)$$

•

$$\dot{q} = \frac{\rho(h) \cdot u^2 \cdot S \cdot c \cdot Cm}{2 \cdot ly \cdot \cos^2(\alpha)} \quad (54)$$

•

$$\dot{\theta} = q \quad (55)$$

To find the unknown values of  $\alpha, \theta$  and  $\delta_e$  the following considerations were made:

- The altitude is from cruise phase of flight so according to the ISA Atmosphere, attached to this document, for 3000 m,  $\rho(h) = \rho(3000 \text{ m}) = 0,909 \text{ Pa}$ .
- The longitudinal velocity is not considered null giving the fact that the airplane can be moving around of himself during hover flight so we consider  $u = 2 \text{ m/s}$ .
- The coefficient of Lift can be found depending on the angle of attack,  $\alpha$ , according to the expression  $C_L = C_{L_0} + C_{L_\alpha} \cdot \alpha + \frac{C}{2V} (C_{L_{\dot{\alpha}}} \cdot \dot{\alpha}) + C_{L_{\delta_e}} \cdot \delta_e$ . According to studies including XFLR5 and Excel:  $C_{L_0} = 0,1257, C_{L_\alpha} = 2,6888 \cdot \alpha + 0,4286, C_{L_{\dot{\alpha}}} = 0,01$ . I assumed that  $\dot{\alpha} = 0$ , as we are considering the equilibrium state. So rewriting the expression we have  $C_L = 0,1257 + 2,6888 \cdot \alpha^2 + 0,4286 \cdot \alpha + 0,01 \cdot \delta_e$
- The coefficient of Drag can be found depending on the angle of attack,  $\alpha$ , according to the expression  $C_D = C_{D_0} + C_{D_\alpha} \cdot \alpha + \frac{C}{2V} (C_{D_{\dot{\alpha}}} \cdot \dot{\alpha}) + C_{D_{\delta_e}} \cdot \delta_e$ . Following the same process that I mentioned above for  $C_L$ , I found the values for  $C_{D_0} = -0,00276, C_{D_\alpha} = 0,3755 \cdot \alpha + 0,00202$ . And we considered that  $C_{D_{\delta_e}} = 0$  because in the equilibrium phase, when you vary the depth control, there is practically no effect on drag. Once more  $\dot{\alpha} = 0$  for the same reason as before. Rewriting the expression we have  $C_D = -0,00276 + 0,3755 \cdot \alpha^2 + 0,00202 \cdot \alpha$ .
- For the throttle fraction we assumed that  $\delta_T = 0,5$ .
- The thrust vector in this case will also be assumed to be null so  $\varepsilon_T = 0$ .
- Given the fact that we are considering the equilibrium state we can consider null the pitch rate (q).
- The Lift is given by the following expression  $L = 0,5 \cdot \rho \cdot v^2 \cdot S \cdot C_L$ . In this case we will consider  $v \approx u = 2 \text{ m/s}$  because we are considering the hover flight and knowing the rest of the data, we have  $L = 0,5 \cdot 0,909 \cdot 2^2 \cdot 10,691 \cdot (0,12578 + 2,688 \cdot \alpha^2 - 0,4286 \cdot \alpha) = 52,244 \cdot \alpha^2 - 8,330 \cdot \alpha + 2,4447$ .
- The pitching moment coefficient can be found based in the next expression  $C_m = C_{m_0} + C_{m_\alpha} \cdot \alpha + \frac{C}{2V} (C_{m_{\dot{\alpha}}} \cdot \dot{\alpha} + C_{m_q} \cdot q) + C_{m_{\delta_e}} \cdot \delta_e$ . Following the same process that I mentioned above for the lift and drag coefficients, I found the values for  $C_{m_0} = -0,0037, C_{m_\alpha} = 0,1635 \cdot \alpha - 0,105$ . For the pitching moment coefficient in relation to the elevator deflection we used the expression  $C_{m_{\delta_e}} = -C_{L_{\delta_e}} \left( \frac{l_H}{c} + \frac{x_{ac} - x_{cg}}{c} \right) = -0,01 \left( \frac{368,07}{2} + \frac{368,07 - 346,07}{2} \right) = -5,411$  and again  $\dot{\alpha} = q = 0$  for the same reason as before. Rewriting the expression, we have  $C_m = -0,0037 + 0,1635 \cdot \alpha^2 - 0,105 \cdot \alpha - 5,411 \cdot \delta_e$ .

## 4.2.2 Lateral-directional Flight

An aircraft is in directional stability when, taken off its flight path, it tends to return immediately to its initial position and is in lateral stability when it remains stable with respect to disturbances around the longitudinal axis of an aircraft, disturbances which involve rolling or yawing. Thus an aircraft is in Lateral-directional flight when:

1. The longitudinal speed is constant, this is,  $u = u_0$ , the vertical speed (up/down) has a constant value,  $w = w_0$ , and the angle of inclination is also constant and equal to  $\theta$ , these values shall be the equilibrium values corresponding to the longitudinal flight before the aircraft starts the Lateral-directional flight;
2. The vertical speed ( $w_0$ ) and the lateral( $v$ ) must be negligible compared to the longitudinal speed ( $u$ );
3. The planing angle ( $\Phi$ ) during the turn takes on a non-zero value during the turn;
4. The skid angle, the angle between the longitudinal axis of the aircraft and the direction in which the aircraft is moving, may be expressed as follows:  $\sin(\beta) = \frac{v}{V}$ . The airspeed is expressed by  $V = \sqrt{u^2 + w^2 + v^2}$ . Using these expressions and taking into account the approximations mentioned above, we obtain for the slip angle:

$$\sin(\beta) = \frac{v}{u_0} \quad (56)$$

As the lateral speed ( $v$ ) must be negligible in relation to the longitudinal speed ( $u_0$ ), the slip angle will be very small, so we can consider that the sine of this same angle can be considered approximately equal to the slip angle ( $\beta$ ) in radians. Then:  $\beta \simeq \frac{v}{u_0}$ .

Therefore for coordinated Lateral-directional flight with small path angle ( $< 10^\circ$ ),  $\beta \simeq 0$  (skid angle at least less than  $3^\circ$ ) and altitude variation we have the following equation:

$$\dot{\psi} = g \cdot \frac{\tan(\Phi)}{V} \cdot \cos(\alpha) \quad (57)$$

Based on the considerations made so far the following equations for Lateral-directional flight then arise:

•

$$\dot{v} = \frac{-QS}{m} \cdot (CD \cdot \sin(\beta) - Cy \cdot \cos(\beta)) + g \cdot \cos(\theta) \cdot \sin(\Phi) - r \cdot u + p \cdot w \quad (\text{com } \beta \simeq \frac{v}{u_0}) \quad (58)$$

•

$$\dot{p} = \frac{Q \cdot S \cdot b}{I_X \cdot I_Z - I_{xz}^2} \cdot (I_z \cdot Cl + I_{xz} \cdot Cn) \quad (\text{with pitch rate } \simeq 0) \quad (59)$$

•

$$\dot{r} = \frac{Q \cdot S \cdot b}{I_X \cdot I_Z - I_{xz}^2} \cdot (I_x \cdot Cn + I_{xz} \cdot Cl) \quad (\text{with pitch rate } \simeq 0) \quad (60)$$

•

$$\dot{\Phi} = p + r \cdot \cos(\Phi) \cdot \tan(\theta_0) \quad (\text{with pitch rate } \simeq 0) \quad (61)$$

Taking into account that  $Q$  is the dynamic pressure ( $0,5 \cdot \rho \cdot V^2$ ),  $b$  is the wingspan,  $I_x, I_z$  and  $I_{xz}$  are the moments of inertia,  $p$  represents the roll rate,  $r$  is the yaw rate,  $\Phi$  is the planing angle and that the pitching rate is neglected because the variation of the pitching angle is approximately zero.

To find the unknown values of  $\delta_r, \phi, p$  and  $r$  made the following considerations:

- The dynamic pressure,  $Q$ , can be obtained from the following expression:

$Q = \frac{1}{2} \cdot \rho \cdot V^2$ , where I have considered the pressure for 3000 m, cruising altitude, which is 0.909 Pascal according to the ISA Atmosphere which is attached to this document. The cruising speed is 100 km/h, which corresponds to 27.78 m/s, which translates into  $Q = \frac{1}{2} \cdot 0,909 \cdot 27,78^2 = 350,75$  Pa.

- The coefficient of Drag can be found using the same expression as in Longitudinal Flight.

- Taking into account that  $\beta$  can be considered null and since the inputs of the control surfaces can also be considered null with the exception of the elevator, that is, the roller and the ailerons will be in their null state, therefore,  $\delta r = 0$  and  $\delta a = 0$ . That said, we can also consider that the derivative of the sideslip coefficient,  $C_{y_s}$ , is null.
- The vertical velocity,  $w$ , can be considered as 0, once we are studying the equilibrium state for the hover phase of flight.
  - As it was said before  $u = 2$  m/s.
- The derivative of the rolling moment coefficient in relation to aileron deflection can be found using the following expression  $C_{l_{\delta a}} = \frac{2 \cdot \tau \cdot (C_{L\alpha})_w}{s \cdot b} \cdot \int_{y_1}^{y_2} c(y) \cdot y \cdot dy$  where:
- $\tau = 0,7$  according to the figure 5 where the effectivity of the flap varies according ratio of the area of the moving part (flap) of the control surface to the total area of the control surface, that we know is 0,5, which means that the effectivity is 0,7.

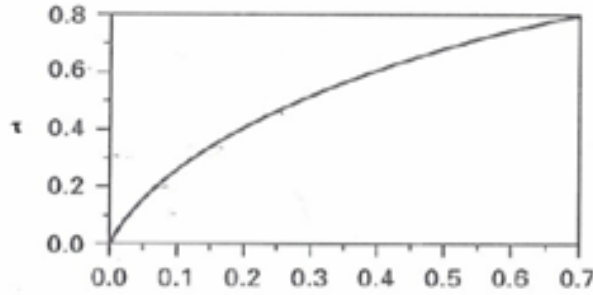


Figure 5: Effectivity of the flap vs Ratio of the area of the moving part (Flap)

- $(C_{L\alpha})_w$  can be considered the same as  $C_{L\alpha}$  because the the wing is considered the main lift surface. As it was described before  $C_{L\alpha} = 2,6888 \cdot \alpha + 0,4286$
- $\int_{y_1}^{y_2} c(y) \cdot y \cdot dy = \int_0^{2,010} 1,317 \cdot y \cdot dy + \int_{2,010}^{3,469} 0,1 \cdot y^2 \cdot dy = 2,66 + 1,12 = 3,78$

So if we rewrite the expression, we will have  $C_{l_{\delta a}} = \frac{2 \cdot 0,7 \cdot (2,6888 \cdot \alpha + 0,4286)}{10,691 \cdot 10,692} \cdot 3,78 = 0,124 \cdot \alpha + 0,0198$

- The derivative of the yaw moment coefficient can be found following the expression  $C_n = C_{n_\beta} \cdot \beta + \frac{b}{2 \cdot V} \cdot (C_{n_p} \cdot p + C_{n_r} \cdot r) + C_{n_{\delta \alpha}} \cdot \delta \alpha + C_{n_{\delta r}} \cdot \delta r$  where
- As before we can consider  $\beta$  as null because it is very small for most of the transport aircrafts, otherwise the aircraft can sideslip.
- $C_{n_p} = C_{n_r} = 0,05$
- $C_{n_{\delta r}} = -(C_{L\alpha})_V \cdot \tau \cdot \frac{S_v}{S} \cdot \frac{l_v}{b} \cdot \eta_v$  with  $(C_{L\alpha})_V = C_{L\alpha}$ , considering that the wing is the main surface of lift,  $\tau = 0,7$  as we saw before,  $\eta_v = -0,06$ ,  $l_v = 0,368$  and  $S_v = 0,334$  m<sup>2</sup>. So if we rewrite the expression we will have  $C_{n_{\delta r}} = -(2,6888 \cdot \alpha + 0,4286) \cdot 0,7 \cdot \frac{0,334}{10,691} \cdot \frac{0,368}{10,692} \cdot (-0,06) = 0,00012 \cdot \alpha + 0,000019$
- $C_{n_{\delta \alpha}}$  can be considered 0.

So rewriting the expression we have  $C_n = \frac{10,692}{2 \cdot 2} \cdot (0,05 \cdot p + 0,05 \cdot r) + (-0,00012 \cdot \alpha - 0,000019) \cdot \delta r = 0,00012 \cdot \alpha \cdot \delta r + 0,000019 \cdot \delta r + 0,1336 \cdot p + 0,1336 \cdot r$ .

- For  $\alpha$  and  $\theta$  we can use the values found before for the Longitudinal Flight.

### 4.2.3 Results

At this stage of the project, I used Matlab software to discover the incognita values mentioned before for each Flight Mode (Longitudinal and Lateral). After finding all the values mentioned before, it was possible to apply a "solve" command in MATLAB to the Flight Dynamics Model Equation.

The procedure previously used to find the equilibrium state was based only on mathematical foundations. However, applying the results to engineering, we concluded that the values obtained are not feasible and cannot be put into practice. Sometimes conventional and purely mathematical solutions do not correspond to reality, since they do not consider the disturbances that a real aircraft may suffer or the use of any type of control. The controller designed in this project will compensate for the fact that this point does not correspond exactly to the ideal equilibrium state.

In engineering terms, it was necessary to apply the loop method to make sure that our solution for the equilibrium state for longitudinal flight is real. In MATLAB this basically translates in using a loop with the cycle "for", where it is possible to restrict the results to certain intervals that correspond with real values for an aircraft of this type.

After the use of the method previously mentioned we obtained the following results:

#### For Longitudinal Flight

- $\alpha = -0.1$  rad
- $\theta = 0.7$  rad
- $\delta_e = -0.07$  rad

#### For Lateral-directional Flight

- $p = 0.004$  rad/s
- $r = -0.008$  rad/s
- $\phi = -0.1$  rad
- $\delta_r = 0$  rad/s

## 4.3 Linearization of Longitudinal and Lateral-directional flight models around a reference control state

### 4.3.1 Longitudinal Flight

For the implementation of the linearization of a longitudinal non-linear flight system using Euler's Method explained before. The functions considered were  $u, \alpha, \theta$  and  $q$  and the vectors as you can see below:

1. State vector:  $x = (u \ \alpha \ \theta \ q)^T$
2. Control vector:  $u_c = (\delta_T \ \delta_e \ \varepsilon_T)^T$
3. Output vector:  $y = (u \ \theta - \alpha)^T$

The specific data used in this linearization can be found at the beginning of this chapter.

The coefficients of Stability and Control follow the below expressions:

- $$C_L = C_{L_0} + C_{L_\alpha} \cdot \alpha + \frac{C}{2V} (C_{L_{\dot{\alpha}}} \cdot \dot{\alpha}) + C_{L_{\delta_e}} \cdot \delta_e \quad (62)$$

- $$C_D = C_{D_0} + C_{D_\alpha} \cdot \alpha + \frac{C}{2V} (C_{D_{\dot{\alpha}}} \cdot \dot{\alpha}) + C_{D_{\delta_e}} \cdot \delta_e \quad (63)$$

- $$C_m = C_{m_0} + C_{m_\alpha} \cdot \alpha + \frac{C}{2V} (C_{m_{\dot{\alpha}}} \cdot \dot{\alpha} + C_{m_q} \cdot q) + C_{m_{\delta_e}} \cdot \delta_e \quad (64)$$

Rewriting  $\dot{u}, \dot{\alpha}, \dot{\theta}$  e  $\dot{q}$  in a standardized way in matrix form and knowing that  $\dot{x} = f(x, u_c) \in \mathbb{R}^4$  :

$$\dot{x} = f(x, u_c) = \begin{bmatrix} \dot{u} & \dot{\alpha} & \dot{\theta} & \dot{q} \end{bmatrix}^T = \begin{bmatrix} f_u(x, u_c) & f_\alpha(x, u_c) & f_\theta(x, u_c) & f_q(x, u_c) \end{bmatrix}^T$$

Where:

- $f_1(x, u_c) = f_u(x, u_c) = \frac{1}{m} \cdot \left(0, 5 \cdot \rho(h) \cdot S \cdot \frac{u^2}{\cos^2(\alpha)}\right) \cdot (CL \cdot \sin(\alpha) - CD \cdot \cos(\alpha) + \delta T \cdot \cos(\varepsilon t)) - g \cdot \sin(\theta) - q \cdot u \cdot \tan(\alpha)$
- $f_2(x, u_c) = f_\alpha(x, u_c) = q + \frac{g \cdot \cos(\alpha)}{u} \cdot \cos(\theta - \alpha) - \frac{\cos(\alpha)}{m \cdot u} \cdot (L - \delta t \cdot \text{Tmá } x \cdot \sin(\varepsilon t) \cdot \cos(\alpha) + \delta t \cdot \text{Tmá } x \cdot \cos(\varepsilon t) \cdot \sin(\alpha))$
- $f_3(x, u_c) = f_\theta(x, u_c) = \frac{\rho(h) \cdot u^2 \cdot S \cdot C \cdot Cm}{2 \cdot I_y \cdot \cos^2(\alpha)}$
- $f_4(x, u_c) = f_q(x, u_c) = \frac{\rho(h) \cdot u^2 \cdot S \cdot C \cdot Cm}{2 \cdot I_y \cdot \cos^2(\alpha)}$

To linearize a system, we need to describe it using a model in the following form:

$\dot{x} = A \cdot x + B \cdot u_c$ , an equation that describes the dynamics of a linear system.

The matrix A is the Jacobian matrix of f in  $(x_r, u_{c_r})$  with respect to the state vector, x. To give an example of this method:  $a_{ij} = \left(\frac{\partial f_i(x, u_c)}{\partial x_j}\right)_{x=x_r; u_c=u_{c_r}}$

In this case we used the central difference method to find the coefficients of matrix A using the following expression and giving the coefficient  $a_{ij}$  as an example:

$$a_{ij} = \frac{f_i(x + h, u_{c_r}) - f_i(x - h, u_{c_r})}{2h} \quad (65)$$

Applying the previous method to MATLAB I wrote all the coefecints with i and j between 1 and 4 for Matrix A. For Matrix B with i between 1 and j between 1 and 2. After that we just need to add the expressions for Matrix A = [A11 A12 A13 A14; A21 A22 A23 A24; A31 A32 A33 A34; A41 A42 A43 A44] and the same for matrix B = [B11 B12; B21 B22; B31 B32; B41 B42]. In the end I used the command "vpa" to increase precision in the output and the results were the following ones:

$$A = 1 \times 10^3 \begin{bmatrix} 0 & -0.5270 & -0.0090 & 0 \\ 0 & 4.6940 & -1.7024 & 0 \\ 0 & 0 & 0 & 0.0010 \\ 0 & -0.0001 & 0 & 0 \end{bmatrix} \quad (66)$$

$$B = 1 \times 10^3 \begin{bmatrix} 5.2510 & -0.0001 \\ -0.519 & 0 \\ 0 & 0 \\ 0 & -0.0026 \end{bmatrix} \quad (67)$$

### 4.3.2 Lateral-directional Flight

Using once more Matlab software and the Central Difference method to linearize the Lateral-directional flight system and considering in this flight model the functions  $\beta, \phi, p, r$ . For the application of this method I made the following considerations: 1. State vector:  $x = (\beta \phi p r)^T$  2. Control vector:  $u_c = (\delta a \delta r)^T$  3. Output vector:  $y = (\beta \phi)^T$

The coefficients of Stability and Control for this type of flight follow the below expressions:

- $$C_n = C_{n_\beta} \cdot \beta + \frac{b}{2 \cdot V} \cdot (C_{n_p} \cdot p + C_{n_r} \cdot r) + C_{n_{\delta_\alpha}} \cdot \delta_\alpha + C_{n_{\delta_r}} \cdot \delta_r \quad (68)$$

- $$C_D = C_{D_0} + C_{D_\alpha} \cdot \alpha + \frac{c}{2 \cdot V} \cdot (C_{D_\dot{\alpha}} \cdot \dot{\alpha} + C_{D_q} \cdot q) + C_{D_{\delta_e}} \cdot \delta_e \quad (69)$$

- $$C_y = C_{y_\beta} \cdot \beta + C_{y_{\delta_a}} \cdot \delta_a + C_{y_{\delta_r}} \cdot \delta_r \quad (70)$$

- $$C_l = \frac{2 \cdot \tau \cdot (C_{L_\alpha})_w}{s \cdot b} \cdot \int_{y_1}^{y_2} c(y) \cdot y \cdot dy \quad (71)$$

Rewriting now  $\dot{\beta}, \dot{\phi}, \dot{p}$  and  $\dot{r}$  in a standardized matrix form and knowing that:

$$\dot{x} = f(x, u_c) \in \mathbb{R}^4$$

where:

$$\dot{x} = f(x, u_c) = (\dot{\beta} \ \dot{\alpha} \ \dot{\theta} \ \dot{q})^T = (f_{\beta}(x, u_c) \ f_{\alpha}(x, u_c) \ f_{\theta}(x, u_c) \ f_r(x, u_c))^T$$

- $f_1(x, u_c) = f_{\beta}(x, u_c)$
- $f_2(x, u_c) = f_{\alpha}(x, u_c)$
- $f_3(x, u_c) = f_{\theta}(x, u_c)$
- $f_4(x, u_c) = f_r(x, u_c)$

For the Lateral-directional Flight we repeated the same process in MATLAB we used for the Longitudinal Flight. Below are the matrices that were obtained for linearizing the system in question where  $\dot{x} = A \cdot x + B \cdot u_c$  :

$$A = \begin{bmatrix} 0.0050 & 4.6840 & -0.1003 & -1 \\ 0 & 0 & 1 & 0.3093 \\ 0 & 0 & 0.3413 & 0.3413 \\ 0 & 0 & 0.0104 & 0.0104 \end{bmatrix} \quad (72)$$

$$B = \begin{bmatrix} 0 & 0 \\ -17.8300 & -17.8300 \\ 0 & 0.0001 \\ 0 & 0.0001 \end{bmatrix} \quad (73)$$

## 4.4 Analysis of the controllability, observability and dynamic stability of the aircraft's longitudinal and Lateral-directional flight

### 4.4.1 Longitudinal Flight

Analysis of the controllability state

A dynamical system is in a controllable state if the system can be guided from one state to another within a finite period of time. In this project we will use the Kalman Characterization, explained next, to understand if the system which is being studied can be considered in a controllable state.

#### **Kalman characterization:**

First let's define the state controllability matrix:

$$\Delta = [ B \ AB \ A^2B \ \dots \ A^{n-1}B ] \quad (74)$$

Then we can discover the characteristic of  $\Delta$  :  $\text{caract}(\Delta) = n$ . If the characteristic of the controllability matrix is equal to  $n$ , the system is controllable.

Using the MATLAB tool, it is possible to calculate this matrix using a single command called "ctrb". Then, using the "rank" command, we can calculate the characteristic of this matrix, nc, which will tell us whether the system is controllable or not. In this case I used this MATLAB commands in the following way:

```
delta = ctrb(A, B);
nc=rank(delta);
```

In the case under study, it was found that both the characteristic of the  $\Delta$  matrix and the dimension of the state vector are equal to 4 , so the system is controllable for the case of longitudinal flight.

#### **Observability Analysis**

To do this analysis we need to start from the theoretical principle mentioned above, the Kalman Mathematical Method, and make the following considerations:

- the state vector can be represented by  $x = (u \ \alpha \ \theta \ q)^T$
- the output vector is expressed by  $y = ( u \ \theta )^T$
- $y$  can be represented as follows  $y = C \cdot x + D$

According to the mathematician Kalman, and considering that C is the output matrix, the observability matrix can be represented by:

$$\Theta = \begin{bmatrix} C \\ CA \\ CA^2 \\ \cdot \\ \cdot \\ \cdot \\ CA^{n-1} \end{bmatrix} \quad (75)$$

In this case we assume that all the variables required for control are measured and real for the aircraft under study. Therefore, it will not be necessary to analyze observability. It is only necessary to analyze observability for the control to work properly when the variables entered as input are not measured. So to conclude, for this specific aircraft in study we assume that the system is observable.

#### Stability Analysis

According to the theoretical model for Theorem 5 (Poincaré-Liapunov), we then calculate the eigenvalues of the state matrix A using the "eig" command in MATLAB and check that they have negative real parts so that we can admit stability of the system for longitudinal flight:  $E = \text{eig}(A)$

We thus obtained the following eigenvalues for Matrix A:

$$\begin{aligned} \lambda_1 &= 4693.835 \\ \lambda_2 &= 0 \\ \lambda_3 &= -0.0000026 + 0.1569i \\ \lambda_4 &= -0.0000026 - 0.1569i \end{aligned}$$

It follows that since there a null eigenvalue, the system is not considered stable.

### 4.4.2 Lateral-directional Flight

#### Analysis of the controllability state

Using the same method as above for longitudinal flight, but this time with the matrices calculated for longitudinal flight, we obtained the characteristic of the  $\Delta$  matrix, i.e. "ctrb(A,B)", which takes the value of

4 as the dimension of the state vector in this case, so the system for Lateral-directional flight is also controllable.

#### Observability analysis

Here the method used should be the same as Longitudinal Flight explained before. As it was mentioned, we used only variables which were measured and real for the aircraft under study so there is no need to do an Observability Analysis for Lateral-directional Flight in this case.

#### Stability Analysis

We calculated the eigenvalues of the A matrix again and followed the same method used for the longitudinal flight, thus obtaining the following values:

$$\begin{aligned} \lambda_1 &= 0.3517 \\ \lambda_2 &= 0.0049 \\ \lambda_3 &= 0 \\ \lambda_4 &= 0 \end{aligned}$$

As we obtained only real values for the eigenvalues of Matrix A, we consider the system as unstable because it has 2 null eigenvalues.

## 4.5 Analysis of the dynamics of the characteristic movements of this aircraft and its flight qualities

The flight qualities of an aircraft can be analyzed based on the dynamics of its characteristic movements. In the case of longitudinal flight, these are the short period and the long period (phugoid) and for Lateral-directional flight they are represented by the spiral, roll and Dutch roll movements. It is the characteristic flight qualities and movements that concern the ease and precision with which the pilot handles this aircraft.

In this chapter we will first perform the necessary calculations for the characteristic movements of the vehicle in question. There are also degrees of stability that we can assign to an aircraft for a certain type of flight. Having said this, we will then need to use the tables indicated earlier in the theoretical model to find out how the aircraft responds to the human pilot's commands, which will lead us to discover the needs of a controller, whose aim is to make up for the deficiencies in the aircraft's flying qualities. The analysis of this degree of stability is mainly related to the aircraft's mission and the phase of flight it is in. Explaining this concept from a more practical point of view, for a military aircraft in combat phase, for example, an exceptional degree of stability is required, while for a commercial aircraft in cruise flight it is possible to let the aircraft be controlled by an autopilot with the supervision of the human pilot.

### 4.5.1 Longitudinal Flight

#### Short and Phugoid Period (or long period)

To calculate these two characteristic movements of the aircraft, we need to take into account the approximate modes of Longitudinal Flight Dynamics mentioned above, and we will follow these steps:

1. We can group the eigenvalues of matrix A for longitudinal flight as follows:

-  $\lambda_1 = a + jb$  and  $\lambda_2 = a - jb$  represent group 1 .

-  $\lambda_3 = c + jd$  and  $\lambda_4 = c - jd$  represent group 2 .

where  $a$  and  $c$  represent the real parts,  $b$  and  $d$  the imaginary parts.

2. Let's now calculate the parameters  $W_n$  and  $\xi$  as follows:

-  $(\lambda_1, \lambda_2) \Rightarrow w_{n_1} = |\lambda_1| = |\lambda_2| \wedge \xi_1 = \frac{-a}{W_{n_1}}$

-  $(\lambda_3, \lambda_4) \Rightarrow w_{n_2} = |\lambda_3| = |\lambda_4| \wedge \xi_1 = \frac{-c}{w_{n_2}}$

3. This is how we calculate the periods themselves (short and long):

-  $T_{p_1} = \frac{2\pi}{w_{n_1} \cdot \sqrt{1-\xi_1^2}}$

-  $T_{p_2} = \frac{2\pi}{w_{n_2} \cdot \sqrt{1-\xi_1^2}}$

4. Finally, we identify which of the periods ( $T_{p_1}$  and  $T_{p_2}$ ) is the short period and the long period, there may be 2 cases:

-  $T_{p_1} > T_{p_2}$  and so  $(\lambda_1, \lambda_2)$  corresponds to the long period and  $(\lambda_3, \lambda_4)$  corresponds to the short period.

-  $T_{p_1} \leq T_{p_2}$  and therefore  $(\lambda_3, \lambda_4)$  corresponds to the long period and  $(\lambda_1, \lambda_2)$  corresponds to the short period.

To implement this method in MATLAB software, a cycle "while" was used to restrict the number of eigenvalues and adapt the logic mentioned before.

The code developed contains:

- first, the matrix E of the values in matrix A which, as I have already mentioned, will be needed to calculate the periods themselves.

- A loop used in programming is called "while" and in this case serves to facilitate the calculation of each of the necessary factors using the fewest lines of code. Only between 1 and 4 since there are only 4 eigenvalues.

-

$$\lambda_n = E(n)$$

to make it easier to identify each of the eigenvalues.

- the "abs" command which calculates the modulus of each eigenvalue.

- the "real" command to select the real part of a number.

- At the end we identify which is the largest, which in this case was 1 , so  $Tp(1)$  corresponds to the long period and  $Tp(2)$  to the short period.

For the longitudinal flight there is no possible solution for the values of the short and long period. That being the case, we can already conclude that the aircraft in study is classified in the worst level for flight quality and will need a robust controller.

To analyze the quality of flight relative to the long period, we need to calculate the minimum time to double the altitude  $T_2 = \frac{\ln(2)}{a}$ , where  $a$  represents the real part of the corresponding eigenvalue. In this case  $T_2$  is not considered as a real number because  $a \approx 0$ , which means that the value of  $T_2$  should be very high and according to the Cooper Harper Scale, shown below in the tables, the phugoid movement is unstable. Therefore, according to the tables 2 and 3, we can say that for longitudinal flight and at the level of phugoid motion, the aircraft has a level 3 for flight quality.

|             |         |                      |
|-------------|---------|----------------------|
| Long Period | Level 1 | $\xi > 0,4$          |
|             | Level 2 | $\xi > 0$            |
|             | Level 3 | $T_2 > 55 \text{ s}$ |

Table 2: Long Period Levels of Quality

|         | Category A and C |              | Category B   |              |
|---------|------------------|--------------|--------------|--------------|
|         | $\xi_{\min}$     | $\xi_{\max}$ | $\xi_{\min}$ | $\xi_{\max}$ |
| Level 1 | 0.35             | 1.30         | 0.3          | 2.0          |
| Level 2 | 0.25             | 2            | 0.2          | 2.0          |
| Level 3 | 0.15             | -            | 0.15         | -            |

Table 3: Short Period Levels of quality

In order to analyze the flight quality for the short period, it is necessary to look at the graph/table that varies  $W_n$  with  $\xi$ , as shown below. Knowing that  $W_n$  and  $\xi$  don't have real solutions in our case we can first say that the short-period movement is not stable and that we are in the unacceptable zone of the table corresponding to the flight quality of the short period in longitudinal flight, which leads *u* to the conclusion that there is a need for a very robust controller for this type of flight.

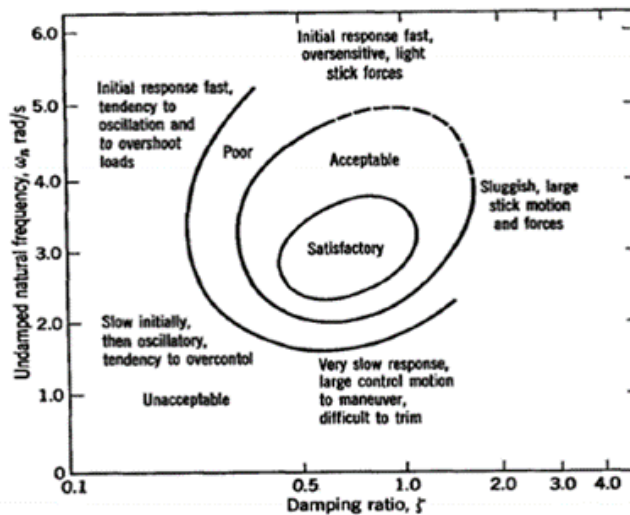


Figure 6: Graphic for the Analysis of the Aircraft Flight Qualities

#### 4.5.2 Lateral-directional Flight

The dynamic characteristics of an aircraft can be determined using the characteristic equation of the A matrix, in this case the Lateral-directional model. Regarding the roots:

1. All roots are real.
2. Two real roots and two complex conjugate roots
3. Two pairs of complex roots (each composed of conjugate roots).

In our case there are only real roots.

From a more modern point of view, the rolling, Dutch rolling and spiral movements can be calculated, identified and analyzed using the eigenvalues of the state matrix A for Lateral-directional flight as follows:

- The spiral motion corresponds to the absolute value of the smallest real eigenvalue;
- Roll corresponds to the absolute value of the largest real eigenvalue, which is always a negative value and is convergent;
- The Dutch Roll corresponds to the real part of the complex eigenvalues.

| Roll (Maximum Time Constant for roll) |          |         |         |         |
|---------------------------------------|----------|---------|---------|---------|
| Class                                 | Category | Level 1 | Level 2 | Level 3 |
| I, IV                                 | A        | 1.0 s   | 1.4 s   | 10 s    |
| II, III                               | A        | 1.4 s   | 3.0 s   | 10 s    |
| Todas                                 | B        | 1.4 s   | 3.0 s   | 10 s    |
| I, IV                                 | C        | 1.0 s   | 1.4 s   | 10 s    |
| II, III                               | C        | 1.4 s   | 3.0 s   | 10 s    |

Table 4: Roll Quality Categories

| Spiral Mode (Minimum time to double an amplitude) |          |         |         |         |
|---|----------|---------|---------|---------|
| Class   | Category | Level 1 | Level 2 | Level 3 |
| I and IV  | A        | 12 s    | 12 s    | 4 s     |
|   | B and C  | 20 s    | 12 s    | 4 s     |
| II and III  | All      | 20 s    | 12 s    | 4 s     |

Table 5: Spiral Mode Quality Categories

In terms of Matlab commands, in order to discover each of these factors, I used a cycle called "for" which allows the program to repeat a set of instructions a certain number of times in order to discover the characteristic movements mentioned above. In this case, we used this cycle to compare each of the real and imaginary parts of the eigenvalues of matrix  $A$  in this particular flight mode, as shown in the following figure.

The results for all the characteristic movements of this aircraft, Roll, Dutch Roll and Spiral were null which means this specific aircraft fits in one of the worst level in terms of flight quality, which can always be solved with a good controller.

Analyzing the flight quality relative to the Roll we can see according to the table  $ABC$ , based on the Cooper-Harper scale, that the Value of Roll doesn't fit this table which means we are in the worst level of Flight Quality.

In order to analyze the Spiral movement, we need to calculate the minimum time to double the amplitude, which would be  $T_2 = \frac{\ln(2)}{\lambda_{\text{spiral}}}$ . As the spiral value in this case is equivalent to 0,12 would be a very high number which is not considered real. Practically speaking we cannot fit this number in the Cooper-Harper scale shown below in table DC.

For the analysis of the Dutch Roll once more we cannot fit our values into the below table which means we are facing the Unacceptable area of the Cooper-Harper Scale.

## 4.6 LQR controller projection

An LQR (Linear Quadratic Regulator) controller allows you to control a linearized system, which in our case can be expressed by:  $\dot{x} = A \cdot x + B \cdot u_c$ . In most cases, a controller is a regulator, but we can say that there are two types of controllers: regulators and followers. A regulator can only follow

| Level    | Category | Class   | $\xi$ min | $\xi \cdot \omega_n$ min<br>[rad/s] | $\omega_n$ min<br>[rad/s] |
|----------|----------|---------|-----------|-------------------------------------|---------------------------|
|          | <b>A</b> | I, IV   | 0.19      | 0.35                                | 1.0                       |
|          |          | II, III | 0.19      | 0.35                                | 0.4                       |
|          | B        | All     | 0.08      | 0.15                                | 0.4                       |
| <b>2</b> | C        | I, IV   | 0.08      | 0.15                                | 1.0                       |
| <b>3</b> |          | II, III | 0.08      | 0.15                                | 0.4                       |

Table 6: Categories of Quality for Dutch Roll

constant references at certain intervals, while for a follower the references don't need to be constant but can vary.

#### 4.6.1 Stabilization for the origin

In order to develop a quadratic controller, it is important to pay attention to the choice of a control vector  $u(t)$  in order to minimize the quadratic performance criterion (J). This is given by:

$$J(u) = \int_0^{\infty} L(x, u_c) dt \quad (76)$$

where  $L(u_c, x)$  is a quadratic function of  $x$  and  $u_c$ .

The control to be determined is intended for linear systems and aims to minimize a quadratic criterion. The resulting control is a linear quadratic regulator, which is also known as an LQR. It is important in these regulators to parameterize the control vector as a linear function of the state vector  $x$  :

$$u_c = -Kx \quad (77)$$

where  $K$  is a matrix with  $m$  rows and  $n$  columns ( $K \in R^{m \times n}$ ). Thus, the previous equation can be written in the following matrix form:

$$\begin{bmatrix} u_1 \\ u_2 \\ \cdot \\ \cdot \\ u_m \end{bmatrix} = - \begin{bmatrix} k_{11} & k_{12} & \cdot & \cdot & \cdot & k_{1n} \\ k_{21} & k_{22} & \cdot & \cdot & \cdot & k_{2n} \\ \cdot & \cdot & \cdot & \cdot & \cdot & \cdot \\ \cdot & \cdot & \cdot & \cdot & \cdot & \cdot \\ k_{m1} & k_{m2} & \cdot & \cdot & \cdot & k_{mn} \end{bmatrix} \begin{bmatrix} x_1 \\ x_2 \\ \cdot \\ \cdot \\ x_n \end{bmatrix} \quad (78)$$

In other words, the design of a controller comes down to determining the matrix  $K$  in order to minimize the performance criterion  $J$  with the control defined by equation (123). Since the expression  $L(x, u_c)$  in equation (321) is quadratic in  $x$  and  $u$ , it can be written in the following form:

$$J(u_c) = \int_0^{\infty} (x^T Q x + u_c^T R u_c) dt \quad (79)$$

where  $Q$  and  $R$  are positively semi-definite real Hermitian or symmetric matrices ( $Q \geq 0; R > 0$ ). Note that the matrix  $Q$  represents a weight assigned to the cost of the states (its variation around its quadratic form), and  $R$  weights the control signal  $u(t)$ . In practice,  $R$  and  $Q$  are defined as follows :

$$Q = \begin{bmatrix} q_1 & 0 & 0 & 0 \\ 0 & q_2 & 0 & 0 \\ 0 & 0 & q_3 & 0 \\ 0 & 0 & 0 & q_4 \end{bmatrix}, R = \begin{bmatrix} r_1 & 0 \\ 0 & r_2 \end{bmatrix}$$

Where  $q_i = \frac{\eta_i}{x_{i,\max}^2}$ ,  $r_i = \frac{\lambda_i}{u_{ci,\max}^2}$  with  $\eta_i \geq 1$  and  $\eta_i, \lambda_i$  may be different for each value. Substituting the expression for  $u_c$  into the equations mentioned above, we obtain respectively:

$$\dot{x} = A \cdot x - B \cdot K \cdot x = (A - B \cdot K)x \quad (80)$$

$$J(u_c) = \int_0^{\infty} (x^T (Q + K^T R K) x) dt \quad (81)$$

The equation for  $\dot{x}$  is the equation for the closed loop system (with the controller running). To determine the control law, it is necessary to find a Lyapunov function  $V$  for the closed loop system of the form closed loop system in the form  $V(x) = x^T P x$ , where  $P$  is a positively dense symmetric matrix. In this case, the derivative in time of this Lyapunov function must be equal to the opposite of the function to be integrated in equation of  $J$ , which means:

$$\dot{V}(x) = \frac{d}{dt} (x^T P x) = -x^T (Q + K^T R K) x \quad (82)$$

But we have:

$$\frac{d}{dt} (x^T P x) = \dot{x}^T P x + x^T P \dot{x} \quad (83)$$

Therefore:

$$x^T [(A - BK)^T P + P(A - BK)] x = -x^T (Q + K^T R K) x \quad (84)$$

For this differential equation to be stable, the matrix K must satisfy the following equation (Lyapunov's):

$$(A - BK)^T P + P(A - BK) = - (Q + K^T R K) \quad (85)$$

Assuming that the matrix K is the unknown in this last equation, then the solution is:

$$K = R^{-1} B^T P \quad (86)$$

So according to the previous equation:

$$u_c = -Kx = -R^{-1} B^T P x \quad (87)$$

Note that in this case, the matrix P in the previous equation must satisfy the following Riccati equation:

$$A^T P + P A - P B R^{-1} B^T P + Q = 0 \quad (88)$$

The analytical solution of  $\dot{x}$  equation is given by:

$$\dot{x} = (A - BK)x = A_c x \rightarrow x = e^{A_c t} x_0, \forall t \quad (89)$$

To simulate the closed loop system (system controlled by the control law  $u_c = -Kx$ ), simply simulate the previous equation using the following formula:

$$x_{K+1} = e^{A_c \Delta t} \times x_k, K \in [0; N] \quad (90)$$

In practice we can dimension the controller by implementing the following algorithm in MATLAB:

- Consider a matrix Q and R as denoted before with arbitrary values of  $\lambda$  and  $\eta$  but so that the matrices are positively semi-definite.
- Find P by the Riccati equation, using the command `lqr(A, B, Q, R)`.
- Substitute P in equation of  $\dot{x}$  to find the optimal control expression ( $u_c = -Kx = -R^{-1} B^T P x$ ) that regulates the system and in fact minimizes the cost function in the equation  $J(u)$ .
- Simulate the analytical solution using MATLAB's `expm(A_c \Delta t)` command to apply in the equation  $x_{K+1}$ .
- Once we have an initial simulation, we can iterate the values of  $\eta_i$  and  $\lambda_i$  until we obtain a controller that stabilizes the system in the desired time interval.

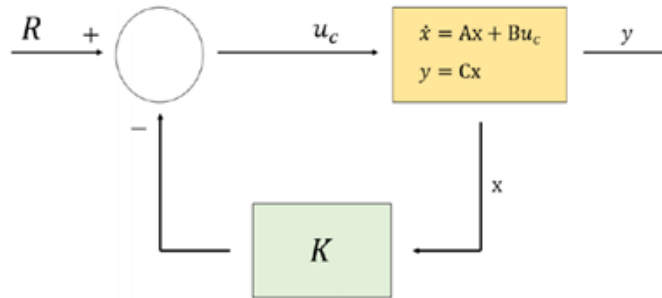


Figure 7: Schematic representation of an LQR controller

## 4.7 Stabilization for outside of the origin

In order to design a controller that stabilizes the aircraft away from the origin, it is necessary to start from a system whose dynamics are described in state space by the following equations a system whose dynamics are described in state space by the following equations:

$$\dot{x} = Ax + Bu_c \quad (91)$$

$$y = Cx \quad (92)$$

To design this controller, it is necessary to assume that the system is controllable, both in terms of state and output. Thus, the aim is to design a controller so that it drives the system towards the reference  $y_{ref}$ . First of all, it is necessary to determine the denoised positive symmetric matrix,  $P$ , which is the solution to the following Riccati equation.

$$A^T P + PA - PBR^{-1}B^T P + Q = 0 \quad (93)$$

In the equation above, the matrix  $Q$  is symmetric and denoised positive and  $R$  is also denoised positive. These matrices are determined in the same way as described in the previous section. The matrix  $P$  can be determined using the LQR method. Once the matrix  $P$  has been obtained, the next step is to create the Lyapunov function, which takes the following form:

$$V(x) = x^T P x \quad (94)$$

The main difference between stabilizing to the origin or away from the origin is that now it is necessary to determine the state  $x$  and the control  $u_c$  that correspond to the output reference  $y_{ref}$  by solving the following system of equations:

$$\begin{cases} x^* = Ax^* + Bu_c^* = 0 \\ Cx^* = y_{ref} \end{cases}$$

This system of equations is equivalent to:

$$\begin{pmatrix} A & B \\ C & 0 \end{pmatrix} \begin{pmatrix} x^* \\ u_c^* \end{pmatrix} = \begin{pmatrix} 0 \\ I \end{pmatrix} y_{ref}$$

So the solution is given by:

$$\begin{pmatrix} x^* \\ u_c^* \end{pmatrix} = \begin{pmatrix} A & B \\ C & 0 \end{pmatrix}^{-1} \begin{pmatrix} 0 \\ I \end{pmatrix} y_{ref}$$

At each instant  $t_k$ , we apply the control signal calculated as follows:

$$u_{c,k} \equiv u_c(t_k) = u_c^* - R^{-1}B^T P(x_k - x^*)$$

where  $x_k \equiv x(t_k)$  is the current state of the system.

After calculating  $x$  and  $u_c$  we can substitute  $u_{c,k}$  and we get :

$$\dot{x} = (A - BK)x + B(Kx^* + u_c^*) \quad (95)$$

On this section we will apply the method only to the Longitudinal Flight.

### 4.7.1 Control of pitch angle and speed

When sizing the LQR controller, the flight qualities must be taken into account. In the case of longitudinal flight, we observed earlier that the flight quality was unacceptable, so a robust controller will be needed.

A controller is said to be robust if it is able to guarantee a certain minimum standard of performance for the overall closed-loop system, even in the presence of uncertainties about the mathematical model of this system, external disturbances acting on it or of this system, external disturbances acting on it or parasitic dynamics present in it. In other words, for our aircraft, a controller should be able to stabilize the system to the desired value in a time period between desired value in a period of time between 5 and 10 seconds, but since we need a robust controller it will have to do so in at least half

|          |   |
|----------|---|
| $\eta_1$ | 3 |
| $\eta_2$ | 3 |
| $\eta_3$ | 3 |
| $\eta_4$ | 3 |

Table 7: Chosen  $\eta$  values

|             |     |
|-------------|-----|
| $\lambda_1$ | 0.5 |
| $\lambda_2$ | 0.5 |

Table 8: Chosen  $\lambda$  values

the time since it will have to take into account the presence of disturbances acting on it during that period of time.

The controller for the longitudinal flight was simulated from the initial instant up to 10 seconds with a  $\Delta t = 0,01s$  and an iteration was made for the values  $\eta_i$  and  $\lambda_i$  until we obtained the system to stabilize in a time period of less than 5 seconds, we obtained the following graphs for the pitch angle and speed.

In order to stabilize the system towards the origin, it is necessary to determine the matrices  $Q$  and  $R$ , the penalty matrices. This is an iterative process since it consists of testing various  $\eta'$ s and  $\lambda'$ s that satisfy the condition, which is that the airspeed and pitch angle stabilize before 5 s. One of the concerns when carrying out this work was to keep the  $\lambda'$ s of the R matrix with the maximum value, 1, since the larger the terms in this matrix, the less energy expended by the system to stabilize the aircraft. Thus, the values of  $\lambda_i$  and  $\eta_i$  chosen are as follows on the Tables 7 and 8.

As we can see, the values of  $\lambda'$ s are high, which means that the matrix  $Q$  is also high. A high  $Q$ -matrix generally means that the poles of the closed loop system are located further to the left in the complex plane, which translates into a faster decay of the system to zero. Based on the values above, the  $Q$  and  $R$  matrices determined are shown below.

$$Q = \begin{bmatrix} 0.02 & 0 & 0 & 0 \\ 0 & 38.54 & 0 & 0 \\ 0 & 0 & 10.68 & 0 \\ 0 & 0 & 0 & 2.72 \end{bmatrix}, R = \begin{bmatrix} 3.13 & 0 \\ 0 & 1.78 \end{bmatrix}$$

The initial conditions for this simulation were:

- $$u_0 = 10m/s \tag{96}$$

- $$a_0 = 0.02 \tag{97}$$

- $$\theta_0 = 0.2 \tag{98}$$

- $$q_0 = 0.5rad/s \tag{99}$$

Once the controller has been designed, we can confirm that the objective has been achieved since both the angle and the longitudinal speed stabilize before the 5 s. Thus, the designed control is robust, just as it needed to be since both the short period and the phugoid showed instability.

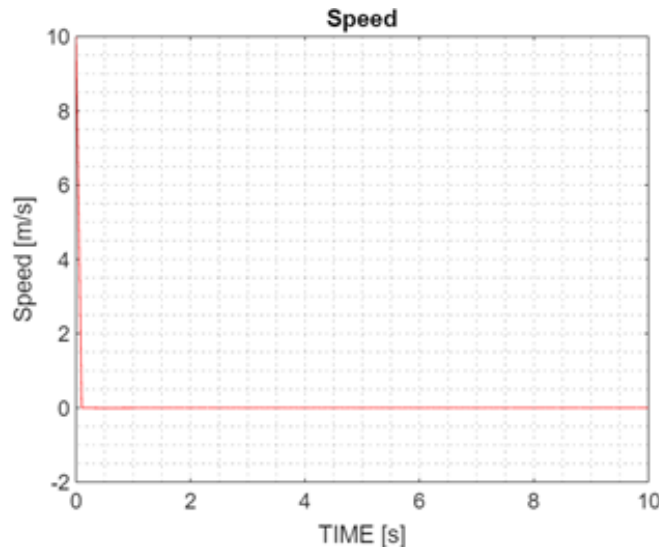


Figure 8: Stabilization of speedwith for the Origin after implementing LQR

Looking at the graphs above for the control of the pitch angle and speedwith the LQR controller, we can see that the values are converging to zero in the case of the stabilization for the origin. For the Stabilization out of the origin there are 3 examples I simulated and in all of them the values are also converging to the chosen reference values ( $u=10$  m/s and  $\theta=0,2$  rad;  $u=11$  m/s and  $\theta=0$  rad;  $u=10,5$  m/s and  $\theta=0,3$  rad) in a time period of less than 5 seconds as assumed.

To be more accurate I did one more simulation for difeerent chosen reference values of  $u$  and  $\theta$  ( $u=6$  m/s and  $\theta=0,2$  rad;  $u=5$  m/s and  $\theta=0,1$  rad;  $u=1$  m/s and  $\theta=0$  rad), which you can see in the figures 12 and 13. For this second simulation it is possible to observe that  $u$  and  $\theta$  are converging as well to the chosen ones in less than 5 seconds. It can therefore be concluded that the controller for longitudinal flight is robust as planned.

After the implementation of the Controller it was possible to analyse once more the flight qualities using the same method as before and now according to the Cooper-Harper Scale we can say that the aircraft is in the Level 2 of Flight Quality.

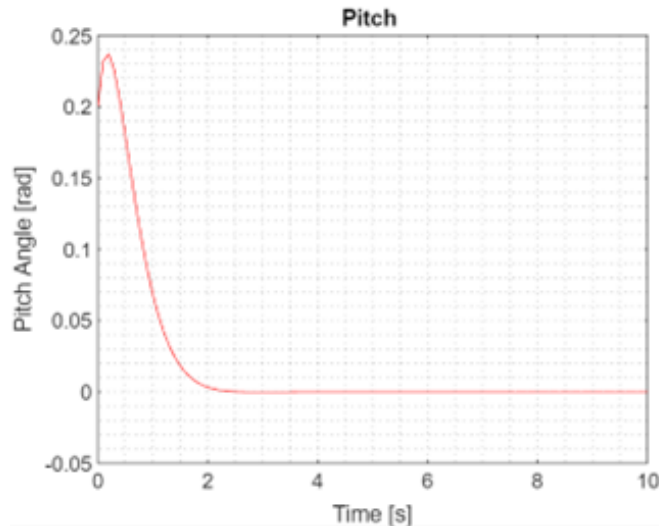


Figure 9: Stabilization of the pitch angle for the Origin after implementing LQR

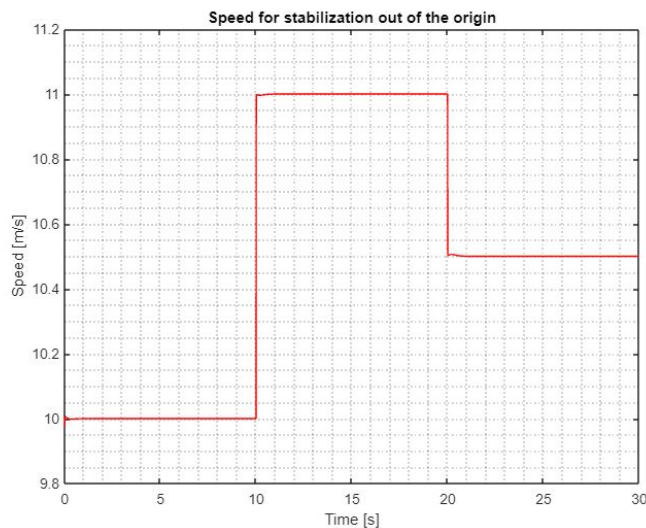


Figure 10: Stabilization of the speed for outside of the Origin after implementing LQR

#### 4.7.2 Analysis of the regulations for VTOL Aircraft from the European and USA Authorities

In recent years, Vertical Takeoff and Landing (VTOL) vehicles have gained significant attention for their potential to revolutionize transportation, logistics, and urban mobility. Whether piloted by humans or operated autonomously, these vehicles represent a new frontier in aviation. To ensure the safe integration of VTOL vehicles into airspace, regulatory agencies such as the European Union Aviation Safety Agency (EASA) and the Federal Aviation Administration (FAA) have developed specific regulations. This chapter explores the regulatory landscape for VTOL vehicles and identifies areas that require improvement to address the unique challenges they pose.

##### Regulations for VTOL Vehicles with Human Pilots

###### 1. EASA's Approach

EASA, as the regulatory authority for aviation safety within the European Union, has implemented a comprehensive set of regulations for VTOL vehicles with human pilots. These regulations, present in [6] encompass various aspects of VTOL operations:

- Certification and Airworthiness: EASA sets rigorous certification requirements for VTOL vehicle manufacturers. Manufacturers must demonstrate compliance with airworthiness standards,

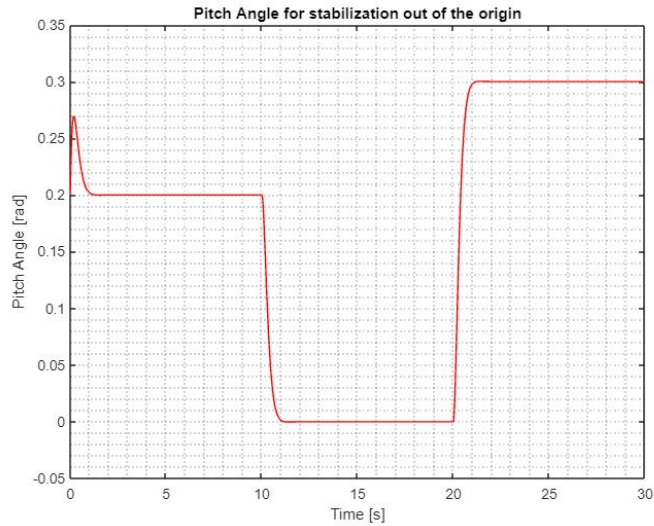


Figure 11: Stabilization of the Pitch Angle for outside of the Origin after implementing LQR

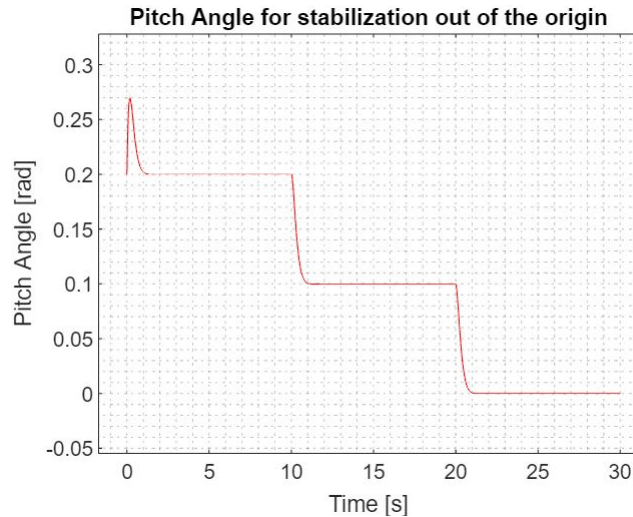


Figure 12: Simulation 2 of Stabilization of the Pitch Angle for outside of the Origin after implementing LQR

including structural integrity, systems reliability, and safety features. These standards ensure that VTOL aircraft meet minimum safety requirements.

- **Pilot Licensing and Training:** Pilots of VTOL vehicles are subject to EASA’s pilot licensing and training standards. These standards cover the specific skills and knowledge required to operate VTOL aircraft safely, including vertical takeoffs and landings, hover operations, and flight in urban environments.
- **Operational Regulations:** EASA’s regulations address operational aspects of VTOL flights. These include rules for flight planning, air traffic management, and safety procedures during takeoff and landing. Special attention is given to VTOL operations in urban areas, where close coordination with local authorities and other airspace users is essential.

## 2. FAA’s Approach

The FAA, responsible for regulating aviation in the United States, also has a framework of regulations in place for VTOL vehicles with human pilots, which you can find in [7]. Key aspects of these regulations include:

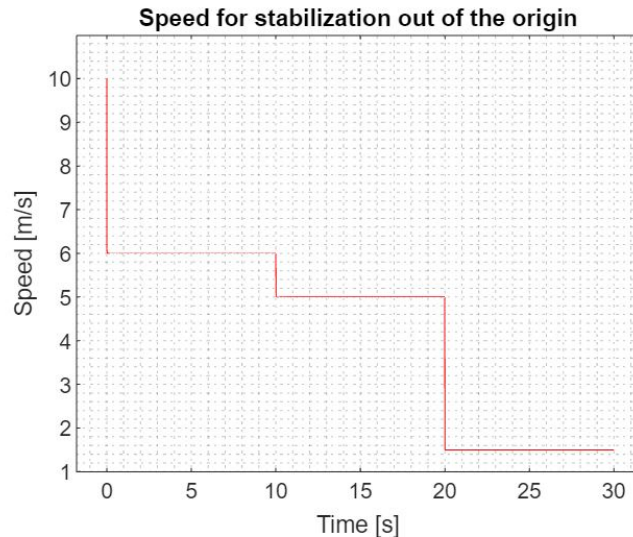


Figure 13: Simulation 2 of Stabilization of the Speed for outside of the Origin after implementing LQR

- Part 23 Regulations: VTOL aircraft designed for human pilots often fall under the FAA’s Part 23 regulations, which govern small transport aircraft. These regulations define airworthiness standards, design requirements, and safety criteria for VTOL vehicles, including tiltrotors and helicopters.
- Part 135 Operations: Operators of VTOL aircraft providing commercial services, such as air taxis, are subject to Part 135 regulations. These regulations cover air carrier certification, maintenance, crew qualifications, and operational safety, ensuring that passengers are transported safely.

### Regulations for VTOL Vehicles without Human Pilots

#### 1. EASA’s Approach

EASA has recognized the growing importance of autonomous VTOL vehicles and has been working to establish regulations for their safe integration:

- Certification of Autonomous Systems: EASA requires manufacturers of autonomous VTOL vehicles to demonstrate the reliability and safety of autonomous flight control systems. This includes redundancy and fail-safe mechanisms to ensure the vehicle can respond to unexpected situations.
- Remote Piloting and Supervision: EASA’s regulations define the requirements for remote piloting and supervision of autonomous VTOL aircraft. These include data link security, real-time monitoring of flight parameters, and protocols for transferring control between remote operators and onboard autonomous systems.

#### 2. FAA’s Approach

The FAA is adapting its regulatory framework to accommodate autonomous VTOL operations:

- Part 107 Regulations: The FAA’s Part 107 regulations for small unmanned aircraft systems (UAS) are relevant to autonomous VTOL operations. These regulations cover pilot certification, operational limitations, and safety standards for autonomous VTOL vehicles used for commercial purposes.
- Advanced Air Mobility (AAM) Regulations: The FAA has been working on developing specific regulations for Advanced Air Mobility (AAM) and Urban Air Mobility (UAM) operations. These regulations will address the unique challenges of autonomous VTOL operations in urban environments, including airspace management and infrastructure requirements.

It's important to note that both EASA and FAA are actively reviewing and updating their regulations to adapt to the rapidly evolving VTOL industry. As VTOL technology continues to advance and becomes more integrated into everyday transportation, these regulatory agencies will likely refine and expand their rules to ensure safety and efficiency in this emerging field. Researchers and industry stakeholders should closely monitor these developments and contribute to the regulatory dialogue to support the responsible growth of VTOL technology.



## 5 Conclusion

In conclusion, this master's thesis has successfully addressed the multifaceted challenges associated with the transition from hover to forward flight for a Vertical Takeoff and Landing (VTOL) Urban Air Mobility (UAM) aircraft, emphasizing three overarching goals: optimizing LQR controllers for VTOL transitions during longitudinal flight, addressing practical implementation challenges, and conducting a comprehensive simulation-based analysis of controller performance.

The investigation into LQR controllers has showed the potential for fine-tuning control strategies during the critical phase of VTOL transition. By optimizing these controllers, we have demonstrated enhanced stability, precision, and efficiency in maneuvering from hover to forward flight. This achievement not only contributes to the theoretical underpinnings of control theory but also establishes a practical foundation for the implementation of robust and adaptive control systems in VTOL UAM aircraft.

The second goal, focusing on practical implementation challenges, has uncovered valuable insights into the real-world constraints and considerations associated with transitioning from hover to forward flight. Factors such as propulsion system dynamics, aerodynamic effects, and sensor limitations have been carefully examined, providing a roadmap for engineers and designers to navigate the intricacies of integrating advanced control algorithms into operational UAM vehicles.

Through a rigorous simulation-based analysis of controller performance, the third goal, this thesis has brought a quantitative assessment of the proposed LQR controllers in a dynamic and evolving flight environment. The simulated scenarios have not only validated the efficacy of the optimized controllers but also offered a platform for sensitivity analysis and scenario-based testing, crucial for anticipating and mitigating potential challenges in real-world applications.

As we reflect on the implications of this research, it becomes evident that the optimized LQR controllers, coupled with a deeper understanding of practical implementation challenges, have the potential to reshape the landscape of VTOL UAM aircraft. The simulation-based analysis serves not only as a validation tool but also as a predictive instrument for assessing controller robustness across diverse operational conditions.

This research represents a significant contribution to the ongoing discourse on urban air mobility. By addressing the specific goals of optimizing LQR controllers, tackling practical implementation challenges, and conducting a thorough simulation-based analysis, we not only expand the theoretical framework but also provide actionable insights for engineers, researchers, and policymakers involved in the development of VTOL UAM systems. The journey toward seamless hover-to-forward-flight transitions continues, and this thesis stands as a pivotal milestone in the pursuit of safe, efficient, and sustainable urban air transportation.

Looking ahead, the goals achieved in this thesis set the stage for continued advancements in the field of UAM. The optimized LQR controllers, informed by practical considerations, provide a solid foundation for further exploration and adaptation. Future research endeavors may extend mainly into the use of the same model for Lateral-directional flight, where it will be able to control the VTOL aircraft for all Flight Modes and make more conclusions about the application of an LQR Controller for a VTOL Aircraft with thrust Vectoring. Another future development of this project may be the application of Gain Scheduling control strategy to this type of controller, experimental validations, real-world testing with all the hardware and software in a small prototype for example, and the integration of additional control features to enhance the adaptability of UAM aircraft in dynamic urban environments such as new infrastructures and processes that will make the VTOL easy and comfortable for everyone.



## References

- [1] Topperly Youtube Channel. Nonlinear control systems. <https://www.youtube.com/playlist?list=PLhdVEDm7SZ-MqSUpBw78Cb2BmI142R2VA>, 2020.
- [2] Burak Yuksek, Aslihan Vuruskan, Ugur Ozdemir, MA Yukselen, and Gökhan Inalhan. Transition flight modeling of a fixed-wing vtol uav. *Journal of Intelligent & Robotic Systems*, 84:83–105, 2016.
- [3] H.K. Khalil. *Nonlinear Systems*. Pearson Education. Prentice Hall, 2002.
- [4] K. Bousson. *Apontamentos de Dinamica e Controlo de Voo, Curso em Mestrado integrado Engenharia Aeronautica, UBI*. 2021.
- [5] J. Roskam. *Airplane Design VII: Determination of Stability, Control and Performance Characteristics: FAR and Military Requirements*. Number v. 1 in Airplane Design. DARcorporation, 1985.
- [6] EASA. Urban air mobility (uam). <https://www.easa.europa.eu/en/domains/drones-air-mobility/drones-air-mobility-landscape/urban-air-mobility-uam>, 2021.
- [7] FAA. Urban air mobility (uam) concept of operations. <http://efaidnbmnnnibpcajpcgclefindmka/jhttps://www.faa.gov/sites/faa.gov/files/Urban2023>.